Article

Immunity

Substance P Release by Sensory Neurons Triggers Dendritic Cell Migration and Initiates the Type-2 Immune Response to Allergens

Graphical Abstract

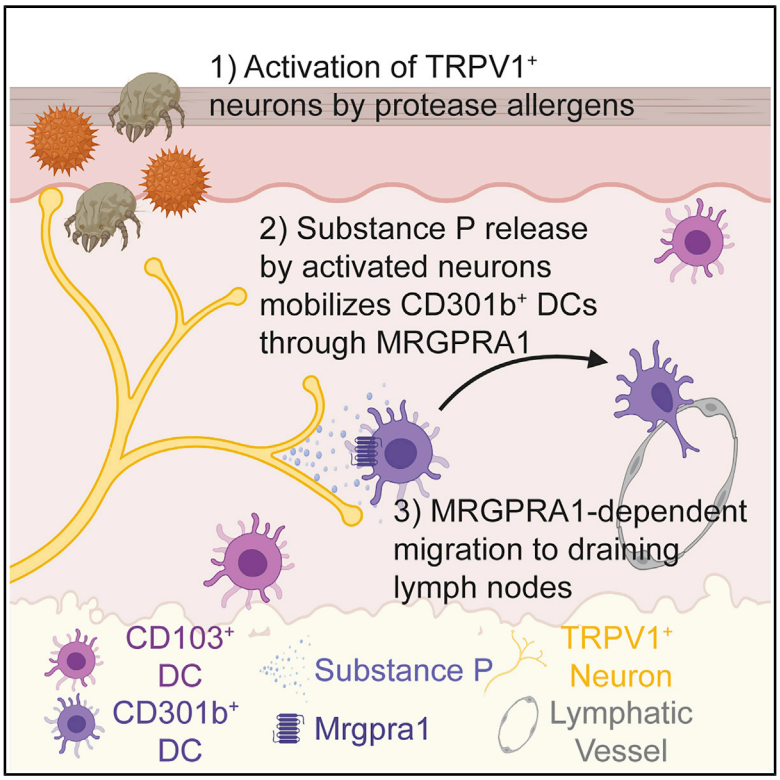

Highlights

- Allergens activate sensory neurons to induce itch responses and Substance P release
- Allergen-activated TRPV1$^+$ neurons trigger CD301b$^+$ DC migration to the lymph node
- Substance P directly induces CD301b$^+$ DC migration through MRGPRA1
- TRPV1$^+$ neurons are required for Th2-differentiation in response to allergens

Authors

Caroline Perner, Cameron H. Flayer, Xueping Zhu, ..., Ohn A. Chow, Isaac M. Chiu, Caroline L. Sokol

Correspondence

clsokol@mgh.harvard.edu

In Brief

Dendritic cells are required for the initiation of the allergic immune response, but it is unclear how they sense allergens. Perner et al. reveal that allergen-induced Substance P release by TRPV1$^+$ sensory neurons triggers MRGPRA1-dependent dendritic cell migration to the lymph node where they initiate the allergic immune response.

Perner et al., 2020, Immunity *53*, 1063–1077
November 17, 2020
https://doi.org/10.1016/j.immuni.2020.10.001

CellPress

Immunity

CellPress

Article

Substance P Release by Sensory Neurons Triggers Dendritic Cell Migration and Initiates the Type-2 Immune Response to Allergens

Caroline Perner,[1,3] Cameron H. Flayer,[1,3] Xueping Zhu,[1,3] Pamela A. Aderhold,[1,4] Zaynah N.A. Dewan,[1,4] Tiphaine Voisin,[2] Ryan B. Camire,[1,2] Ohn A. Chow,[1] Isaac M. Chiu,[2] and Caroline L. Sokol[1,5,*]

[1]Center for Immunology and Inflammatory Diseases, Division of Rheumatology, Allergy and Immunology, Massachusetts General Hospital, Harvard Medical School, Boston, MA 02114, USA

[2]Department of Immunology, Harvard Medical School, Boston, MA 02115, USA

[3]These authors contributed equally

[4]These authors contributed equally

[5]Lead Contact

*Correspondence: clsokol@mgh.harvard.edu

https://doi.org/10.1016/j.immuni.2020.10.001

SUMMARY

Dendritic cells (DCs) of the cDC2 lineage initiate allergic immunity and in the dermis are marked by their expression of CD301b. CD301b$^+$ dermal DCs respond to allergens encountered *in vivo*, but not *in vitro*. This suggests that another cell in the dermis may sense allergens and relay that information to activate and induce the migration of CD301b$^+$ DCs to the draining lymph node (dLN). Using a model of cutaneous allergen exposure, we show that allergens directly activated TRPV1$^+$ sensory neurons leading to itch and pain behaviors. Allergen-activated sensory neurons released the neuropeptide Substance P, which stimulated proximally located CD301b$^+$ DCs through the Mas-related G-protein coupled receptor member A1 (MRGPRA1). Substance P induced CD301b$^+$ DC migration to the dLN where they initiated T helper-2 cell differentiation. Thus, sensory neurons act as primary sensors of allergens, linking exposure to activation of allergic-skewing DCs and the initiation of an allergic immune response.

INTRODUCTION

Allergic diseases are characterized by inappropriate type-2 immune responses targeted against non-infectious environmental antigens and venoms. Defective cutaneous barriers permit the entry of food and environmental allergens into the body where they can ultimately activate the immune system, but the precise mechanisms by which allergens are sensed by the innate immune system remain unclear (Strid et al., 2004). Dendritic cells (DCs) are innate immune cells that link pathogen sensing with adaptive immune activation. Immature DCs actively sample their environment for evidence of pathogens that are detected through their pattern recognition receptors (PRRs). Upon PRR ligation, DCs undergo a complex process of maturation that culminates in their migration to the draining lymph node (dLN), where they present antigen and provide costimulation to naive T cells. Thus, DCs link innate immune sensing with adaptive immune activation.

Conventional DCs (cDCs) can be divided into two main subsets based on transcription factor dependence and functional characteristics. cDC1s are dependent upon interferon regulatory factor 8 (IRF8) and are specialized in antigen cross-presentation, whereas cDC2s are dependent upon interferon regulatory factor 4 (IRF4) and are specialized in T helper cell differentiation. T helper-2 (Th2) cell-skewing cDC2s are dependent upon both IRF4 and Kruppel-like factor 4 (KLF4), and in the skin, this population is characterized by its surface expression of CD301b. CD301b$^+$ DCs migrate to the dLN and are required for Th2 cell differentiation after cutaneous exposure to allergens and helminth parasites (Gao et al., 2013; Kumamoto et al., 2013; Tussiwand et al., 2015). In the type-1 immune response to bacteria and viruses, DC maturation is marked by the upregulation of the chemokine receptor CCR7. This CCR7 upregulation acts in the fashion of a molecular switch, endowing the mature DC to sense and migrate toward gradients of the chemokine CCL21 that are homeostatically produced by the lymphatic endothelium (Ohl et al., 2004). Although cutaneous allergen exposure leads to CCR7-dependent CD301b$^+$ DC migration from the skin to the dLN, it does not lead to CCR7 upregulation (Sokol et al., 2018). In the absence of this molecular switch, what is the primary signal that initiates CD301b$^+$ DC migration out of the skin in response to allergens? Similarly, although CD301b$^+$ DCs are activated by allergens *in vivo* and required for Th2 cell differentiation, CD301b$^+$ DCs exposed to allergens *in vitro* are incapable of promoting Th2 cell differentiation *in vitro* or after *in vivo* transfer (Kumamoto et al., 2013). How do CD301b$^+$ DCs sense allergens *in vivo*?

Type-2 immunogens are a varied group of simple protein allergens, secreted molecules from helminth parasites, and venoms (Palm et al., 2012). Many immunodominant type-2 immunogens

share in common intrinsic or induced enzymatic activity that is required for their immunogenicity, but how they activate the innate immune system is unclear (Lamhamedi-Cherradi et al., 2008; Palm et al., 2013; Porter et al., 2009; Sokol et al., 2008; Van Dyken and Locksley, 2018). Instead of direct detection, DCs may detect endogenous alarmins that are released in response to allergen exposure. Enzymatically active allergens, such as cysteine proteases, induce the release and activation of innate alarmins such as interleukin-33 (IL-33) and thymic stromal lymphopoietin (TSLP) (Cayrol et al., 2018; Tang et al., 2010). Indeed, DCs express the IL-33 receptor ST2, and IL-33 stimulation of DCs can promote Th2 cell skewing (Rank et al., 2009). IL-33 can also stimulate innate lymphoid cells, which can indirectly enhance DC migration to dLNs (Halim et al., 2014). Likewise, TSLP is produced by epithelia in the setting of chronic allergic inflammation and promotes DC activation (Liu et al., 2007). However, data from alarmin-deficient models show only a partial role for alarmins in allergen-induced DC migration and activation (Besnard et al., 2011; Halim et al., 2014). This led us to hypothesize the existence of a primary cellular sensor of allergens that not only senses the presence of allergens but also relays critical cues to initiate the migration of allergic, or Th2 cell-skewing, CD301b$^+$ DCs to the dLN.

One potential allergen sensor is the sensory nervous system, which is highly concentrated in barrier epithelia, broadly responsive to many different stimuli, and directly activated *in vitro* by diverse enzymatically active allergens such as bee venom, house dust mites (HDM), and papain (Chen and Lariviere, 2010; Reddy and Lerner, 2010; Serhan et al., 2019; Talbot et al., 2016; Trier et al., 2019; Veiga-Fernandes and Mucida, 2016). Sensory neurons have been shown to be closely associated with Langerhans cells in the human epidermis, and activation of corneal sensory neurons can lead to DC activation in the contralateral eye (Guzmán et al., 2018; Hosoi et al., 1993). Based on this, we hypothesized a two-step model for allergen activation of DCs wherein allergens activate sensory neurons leading to their local release of neuropeptides (step 1), which then act upon local DCs to promote their migration (step 2) to the dLN where they can activate naive T cells to promote Th2 cell differentiation. Using the model cysteine protease allergen papain, we found that papain induced an immediate sensory response in naive mice. Papain directly activated a subset of sensory neurons that are enriched in TRPV1$^+$ neurons to release Substance P (SP). SP then acted on proximally located Th2 cell-skewing dermal CD301b$^+$ DCs through their expression of a SP receptor *Mrgpra1* to promote their migration to the dLN. Depletion of TRPV1$^+$ neurons, inhibition of sensory neuronal activation, or ablation of *Mrgpra1* from CD301b$^+$ DCs led to a defect in CD301b$^+$ DC migration and as a direct consequence, Th2 cell differentiation. Thus, sensory neurons play an essential role in allergen recognition, DC activation, and initiation of the allergic immune response.

RESULTS

Allergens Induce Immediate and Transient Itch Responses in Naive Mice

To investigate the role of sensory neurons in allergen recognition *in vivo*, we utilized the model allergen papain that induces robust CD301b$^+$ DC migration, Th2 cell differentiation, and immunoglobulin E (IgE) production with defined kinetics after one cutaneous exposure to the enzymatically active allergen (Kumamoto et al., 2013; Sokol et al., 2008). Intradermal (i.d.) papain injection of mice led to an immediate and transient mixed itch (scratching bouts) and pain (wiping bouts) response that was dependent on its protease activity (Figures 1A–1D). Papain-induced sensory responses were overall comparable to the established itch and pain triggers, histamine and capsaicin, respectively (Figures 1A–1D). The sensory response was not specific to papain, because Alternaria extract also induced an itch response (Figure 1A). To investigate what neurons were involved in the sensory response to allergens, we co-injected papain with the lidocaine derivative QX314 that blocks sodium channel activation of neurons after entering through large-pore cation channels including TRPV1 and TRPA1 (Binshtok et al., 2007; Roberson et al., 2013). Co-injection of papain and 1% QX314 blocked the allergen-induced sensory response (Figure 1E and F), suggesting a role for TRPV1$^+$ neurons in direct allergen sensing.

Allergens Directly Activate a Population of Sensory Neurons Enriched in TRPV1$^+$ Neurons

The cell bodies of cutaneous sensory neurons are contained in dorsal root ganglia (DRG) adjacent to the spinal cord. To test whether papain could directly activate sensory neurons, we performed calcium (Ca^{2+}) flux analysis of cultured DRG neurons in response to sequential exposure with different stimuli. Papain induced robust Ca^{2+} influx in DRG neurons within seconds of administration (Figures 2A and 2B). Using potassium chloride (KCl) responsiveness as a marker of live neurons, we found that ~16% of neurons were responsive to papain (Figure 2C), a similar value to that reported for HDM responsive neurons (Serhan et al., 2019). TRPV1 expression defines a subset of nociceptive neurons that not only sense noxious heat, but also promote pruriceptive responses. TRPV1$^+$ neurons are directly activated by HDM cysteine protease allergens and have been associated with allergic inflammation (Roberson et al., 2013; Serhan et al., 2019; Talbot et al., 2015; Tränkner et al., 2014). If the papain responsive neurons were enriched in TRPV1$^+$ neurons, we would expect to see a greater percentage of TRPV1$^+$ neurons in this group. Indeed, whereas capsaicin-responsive neurons (TRPV1$^+$) made up ~35% of the total neurons, they represented an average of 68% of the papain-responsive neurons (Figures 2C–2E). A minority of papain-responsive neurons were also activated by the itch-inducing ligands histamine and/or chloroquine, suggesting that papain-responsive neurons are a heterogeneous population of previously described NP2, NP3, and PEP1 sensory neuron subclasses (Figures 2D and 2E) (Usoskin et al., 2015). Given that papain-responsive neurons strongly overlapped with TRPV1$^+$ (capsaicin-responsive) neurons, we next asked whether the papain-induced sensory response would be affected by depletion of noxious heat-sensing TRPV1$^+$ neurons. Diphtheria toxin (DT) injection into *Trpv1*^{DTR} mice, which express the human diphtheria toxin receptor (DTR) under control of the *Trpv1* promoter, specifically depletes TRPV1$^+$ neurons in the DRG and vagal ganglia (Baral et al., 2018; Pogorzala et al., 2013; Tränkner et al., 2014). Consistent with depletion of TRPV1$^+$ neurons, DT-treated *Trpv1*^{DTR} mice lost their tail flick response to noxious heat and *Trpv1* gene expression in the DRG (Figures 2F and 2G). Deletion of *Trpv1*$^+$ neurons led to a loss of the itch response and a partial block in the pain response

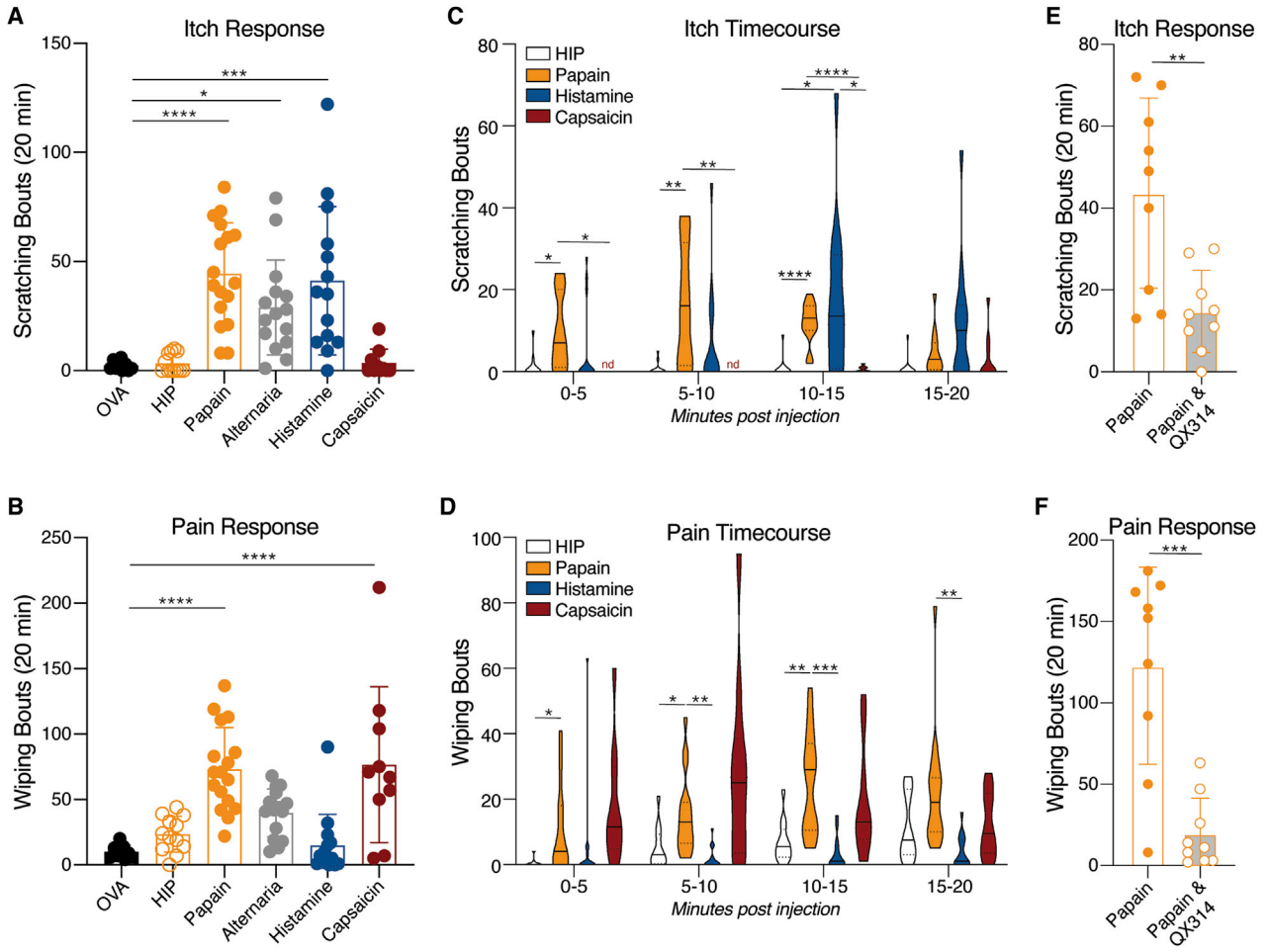

Figure 1. The Protease Allergen Papain Induces an Immediate Sensory Response

(A and B) Wild-type (WT) mice were intradermally (i.d.) injected with ovalbumin (OVA), heat-inactivated papain (HIP), papain, Alternaria extract, histamine, or capsaicin. The total number of ipsilateral cheek (A) scratch events or (B) wipe events.

(C and D) Time course of (C) scratch or (D) wipe events in 5-min increments.

(E and F) Total scratch (E) and wipe (F) events after indicated i.d. injection.

Symbols represent individual mice (A, B, E, and F), bars indicate mean, and error bars indicate SEM. Violin plots (C and D) show grouped time course data from (A and B); line indicates median, dotted lines indicate quartiles, and nd indicates not detected. Statistical tests: ordinary one-way ANOVA with multiple comparisons (A and B), two-way ANOVA with multiple comparisons (C and D), and unpaired t test (E and F). *p < 0.05, **p < 0.01, ***p < 0.001, ****p < 0.0001. Data are representative of at least three independent experiments combined with each experiment including 3–5 mice per group.

to papain (Figures 2H and 2I), indicating that papain activates TRPV1$^+$ neurons *in vitro* and *in vivo*.

Dendritic Cells Do Not Directly Respond to the Cysteine Protease Allergen Papain

DCs directly detect bacterial and viral pathogen-associated molecular patterns (PAMPs) through their direct binding to DC PRRs. This leads to DC maturation, marked by the upregulation of antigen presentation, costimulatory molecules, and CCR7. Thus, maturation promotes the migration of DCs with unique T cell activating capability to the dLN. Consistent with the direct activation of DCs by PAMPs, CD301b$^+$ DCs exposed to lipopolysaccharide (LPS) *in vivo* or *in vitro* upregulated the activation markers PDL2, CD86, and MHC class II (Figures 3A, 3B, and S1A–S1D). Papain immunization induced PDL2 upregulation, but *in vitro* papain stimulation at concentrations up to 100 μg/mL had no effect on PDL2, CD86, or MHC class II expression on CD301b$^+$ DCs (Figures 3A, 3B, and S1A–S1E). At higher concentrations, overnight papain stimulation led to a decrease in PDL2 and CD86 expression possibly due to proteolytic cleavage (Figure S1E). Immunization with papain and LPS also led to an increase in the chemotactic activity of CD301b$^+$ DCs (Figure 3C), whereas *in vitro* exposure with papain had no effect (Figure 3D). These observations suggest that DCs do not independently detect allergens.

CD301b$^+$ Dendritic Cells Colocalize with Sensory Neurons

Given our observations that sensory neurons, but not DCs, are directly activated by allergens, we hypothesized that allergens are detected by sensory neurons that then relay this signal to local DCs. To determine whether sensory neurons could be

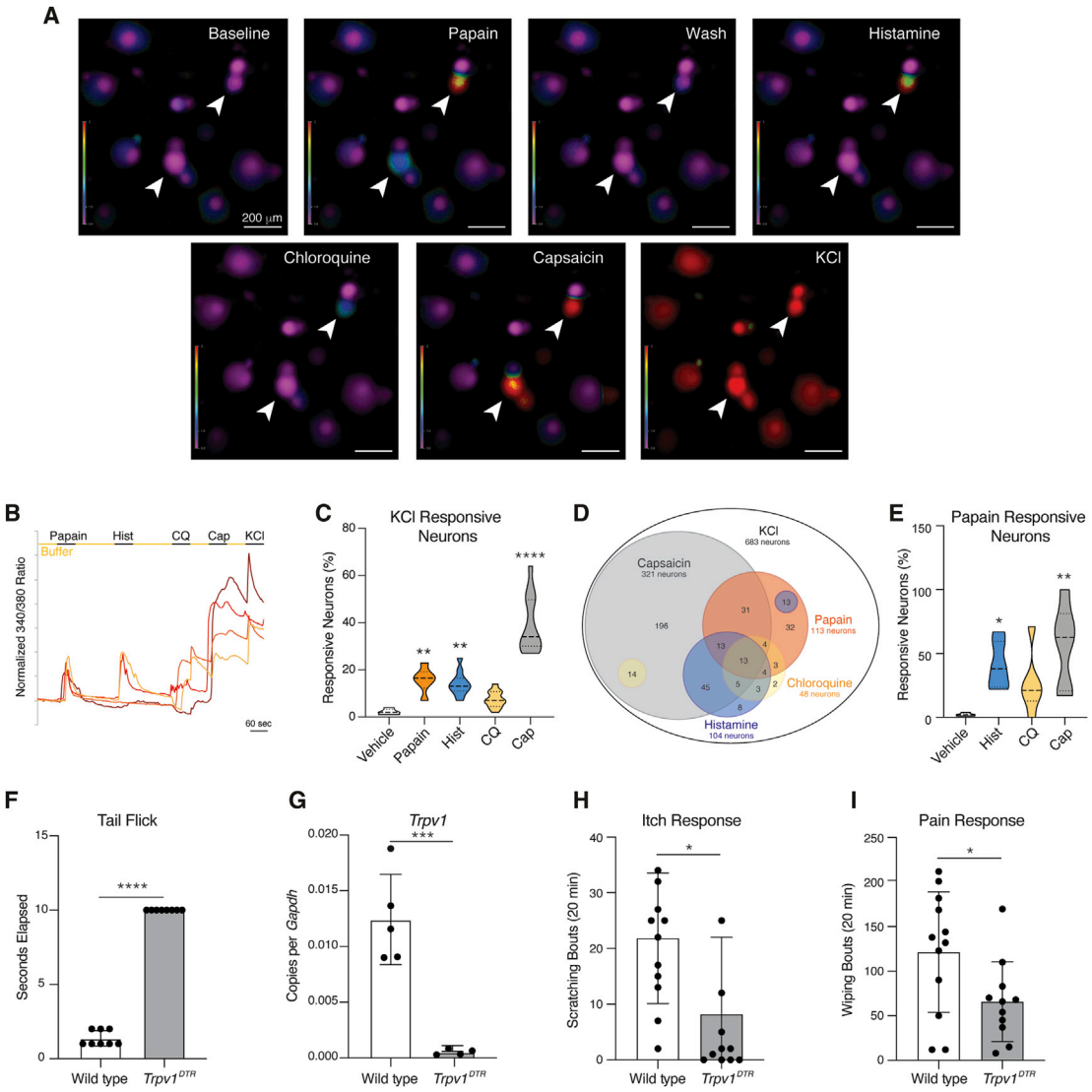

Figure 2. TRPV1$^+$ Neurons Are Directly Activated by Papain and Are Required for the Papain-Induced Sensory Response

(A) Representative Fura-2-AM ratiometric fields of cultured DRG neurons at baseline and after sequential treatment as shown with wash steps in between all stimuli.

(B) Calcium (Ca^{2+}) traces of representative DRG neurons (colored separately for identification) treated as in (A).

(C) The percent of total excitable (KCl responsive) DRG neurons that responded to the indicated treatments.

(D) Venn diagram showing responsiveness of individual DRG neurons.

(E) The percent of papain responsive DRG neurons that also responded to the indicated stimuli as compared to the total vehicle responsive neurons. (C–E) Data were calculated from 12 fields of view and 1,389 neurons that were sequentially stimulated with papain (6 fields of view and 705 neurons) or vehicle (6 fields of view and 684 neurons) followed by histamine, chloroquine, capsaicin, and KCl.

(F) Tail flick assay of WT or *Trpv1*^{DTR} mice intraperitoneally injected with DT.

(G) QPCR analysis of *Trpv1* from DRG of DT treated WT or *Trpv1*^{DTR} mice.

(H and I) Total scratching (H) or wiping (I) events in DT-treated WT or *Trpv1*^{DTR} mice after papain injection. Symbols represent individual mice (F–I), bar indicates mean, and error bars indicate SEM. Violin plot (C and E) lines indicate median, dotted lines indicate quartiles. Statistical tests: ordinary one-way ANOVA with multiple comparisons (C and E), unpaired t test (F–I). *$p < 0.05$, **$p < 0.01$, ***$p < 0.001$, ****$p < 0.0001$. Data are representative of at least three independent experiments combined with each experiment including 3–5 mice per group.

physically interacting with CD301b$^+$ DCs *in vivo*, we imaged the naive skin of *Nav1.8*$^{cre/+}$*tdTomato*^{loxSTOPlox} reporter mice (*Nav1.8*^{tdTomato}) where *Nav1.8*-lineage nociceptive sensory neurons are marked by tdTomato expression (Stirling et al., 2005). CD301b$^+$ DCs were localized in close proximity to the Nav1.8$^+$ nerve fibers in the naive dermis (Figure 3E). Furthermore, CD301b$^+$ DCs were significantly closer to sensory neurons than were their CD301b$^-$ counterparts, which in the dermis include the Th1 cell-skewing cDC1 and the Th17 cell-skewing subset of cDC2 (Figure 3F). Given these observations, as well as the known interplay between sensory neurons and CD301b$^+$ DCs in Candida infection (Kashem et al., 2015), we hypothesized

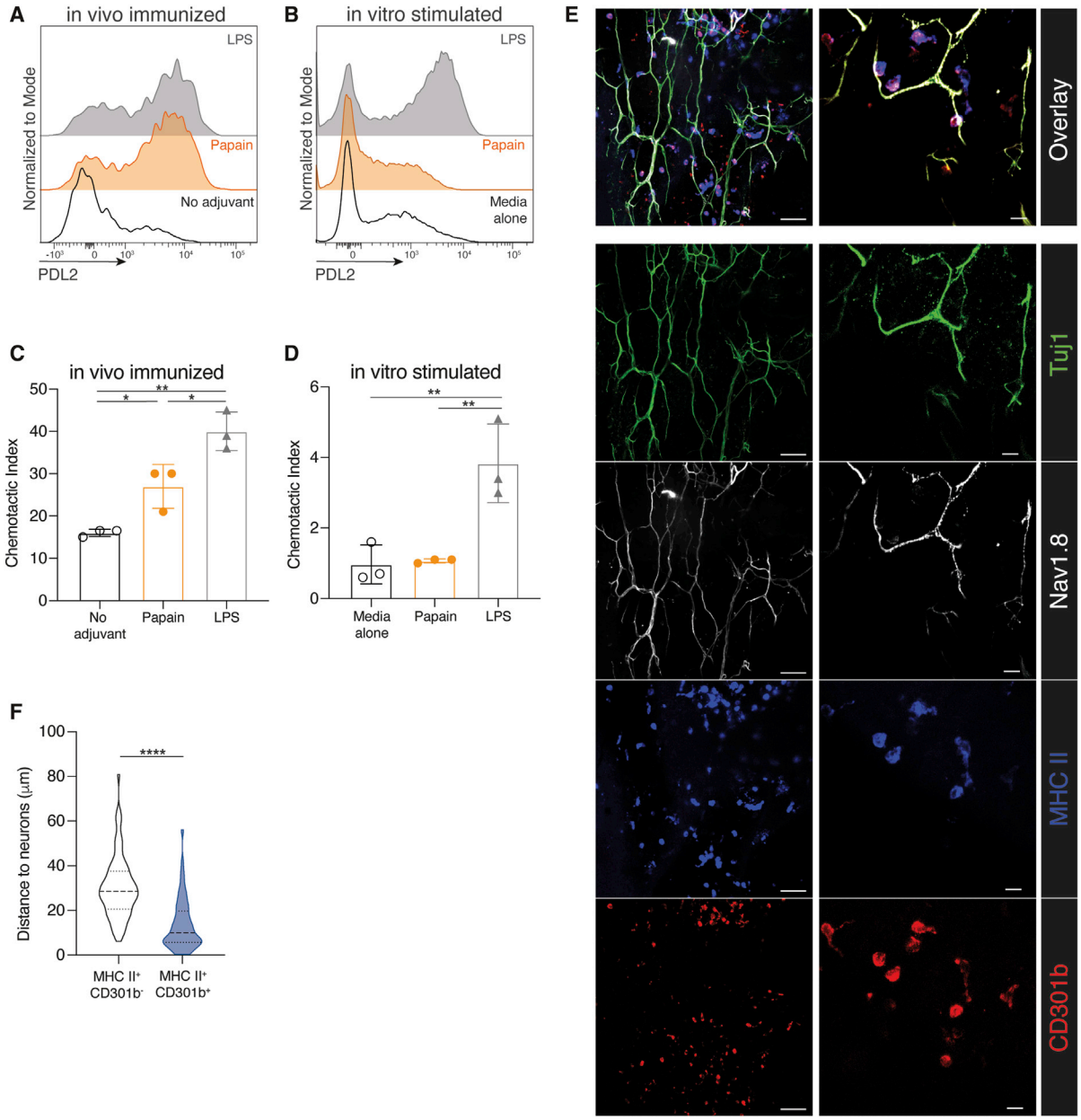

Figure 3. CD301b$^+$ Dendritic Cells Do Not Respond Directly to the Protease Allergen Papain and Are Found in Close Proximity to Sensory Neurons in the Dermis

(A) Flow cytometry of PDL2 expression on live CD11c$^+$CD301b$^+$ DCs from the dLN 24 h after i.d. immunization with OVA (No adjuvant), OVA and papain (Papain), or OVA and LPS.

(B) Flow cytometry of PDL2 expression on live CD11c$^+$CD301b$^+$ BMDCs after overnight stimulation with media, papain, or LPS.

(C and D) Transwell migration to CCL21, normalized to media only control (chemotactic index), of (C) CD11c$^+$CD301b$^+$ cells sorted from the dLN of mice immunized as in (A) or of (D) BMDCs stimulated as in (B).

(E) Confocal immunofluorescence microscopy of naive dermal sheets from *Nav1.8^{tdTomato}* (white) mice stained with Tuj1 (green), MHCII (blue), and CD301b (red). Scale bar in left 20× panels shows 50 μm, scale bar in right 63× panels shows 10 μm.

(F) Closest distance (μm) between MHCII$^+$CD301b$^-$ (white, n = 81) and MHCII$^+$CD301b$^+$ (blue, n = 122) cells and tdTomato$^+$ neurons from naive *Nav1.8^{tdTomato}* mice (10 fields of view). Symbols represent individual replicates (C and D). Bars indicate mean and error bars indicate SEM. Solid lines on violin plots (F) indicate median, dotted lines indicate quartiles. Statistical tests: ordinary one-way ANOVA with multiple comparisons (C and D), unpaired t test (F). *$p < 0.05$, **$p < 0.01$, ***$p < 0.001$, ****$p < 0.0001$. Data are representative of at least three experiments (A–F), combined in (F) with each experiment including 2–5 mice per group. See also Figure S1.

that the spatial relationship between sensory neurons and CD301b$^+$ DCs could reflect a functional requirement for neuronal stimulation specific to allergen-responsive CD301b$^+$ DCs in the dermis.

TRPV1$^+$ Sensory Neuron Activation Is Required for Allergen-Induced CD301b$^+$ DC Migration

We hypothesized that sensory neurons, activated by allergens, may relay a signal to closely associated CD301b$^+$ DCs to activate their allergen-induced migration to the dLN. To assess allergen-induced CD301b$^+$ DC migration, we used Kaede mice that express a photoconvertible green to red fluorescent protein, which allows the tracking of cells originating from the site of photoconversion and allergen exposure (Kaede^{red}) (Tomura et al., 2008). As previously described, papain immunization led to a specific migration of CD301b$^+$ DCs from the photoconverted skin to the dLN (Figure 4A) (Sokol et al., 2018). QX314 co-injection blocked this papain-induced migration of skin emigrant, Kaede^{red}, CD301b$^+$ DCs to the dLN (Figure 4A), suggesting a role for sensory neuron activation in CD301b$^+$ DC migration *in vivo*. To evaluate possible DC-specific effects of QX314 we performed *in vitro* chemotaxis assays of bone marrow-derived DCs (BMDCs). Although higher concentrations inhibited migration, 1% QX314 had no effect on BMDC migration *in vitro*, indicating a specific role for neurons in allergen-induced DC migration (Figure 4B).

Given our data that papain activated a population of neurons enriched in TRPV1$^+$ sensory neurons (Figures 2D, 2E, 2H, and 2I), we hypothesized that TRPV1$^+$ neurons would be required for papain-induced CD301b$^+$ DC migration. We generated Kaede × *Trpv1*^{DTR} mice and performed DT-mediated depletion of *Trpv1*$^+$ neurons. To evaluate the specificity of *Trpv1*^{DTR}-mediated depletion, we first assessed *Trpv1* expression in a published murine skin single-cell RNA sequencing (scRNA-seq) dataset as well as in cutaneous immune cells from the Immunological Genome Consortium (Immgen) microarray dataset and found no *Trpv1* expression in these cells (Figures S2A and S2B) (Heng et al., 2008; Joost et al., 2020). We next verified this by examining the frequency of cutaneous immune cells after DT-mediated depletion. Although mice depleted of TRPV1$^+$ cells showed a significant increase in total DCs and mast cells, there was no decrease in percentage of immune cell subsets in the skin, illustrating the specificity of *Trpv1*^{DTR} depletion for sensory neurons in the skin (Figure S2C). Although there was no difference in dLN cellularity, papain-immunized Kaede × *Trpv1*^{DTR} mice showed a loss of Kaede^{red} CD301b$^+$ DCs in the dLN compared with Kaede mice (Figures 4C and 4D). TRPV1$^+$ neuronal depletion had no effect on the frequency or number of CD301b$^+$ DCs in the naive dermis (Figure 4E), indicating that disrupted CD301b$^+$ DC migration to the dLN was due to a specific defect in papain-induced migration. Alternaria extract similarly led to CD301b$^+$ DC migration from the skin to the dLN that was blocked by QX314, indicating that sensory neuron activation may be a global requirement for allergen-induced CD301b$^+$ DC migration (Figure 4F). This requirement for sensory neuron activation was specific to allergen-induced CD301b$^+$ DC migration. There was no effect of QX314 on the migration of CD103$^+$ DCs (including cDC1 and Th17 cell-skewing cDC2s in the dermis) after immunization with OVA and LPS (Figure 4G).

Substance P Release from Sensory Neurons Induces CD301b$^+$ DC Migration

Our data suggested that TRPV1$^+$ sensory neurons directly sense cysteine protease allergens and relay signals to promote the egress of local Th2 cell skewing CD301b$^+$ DCs to the dLN. Activated peptidergic TRPV1$^+$ neurons can release SP in response to allergen exposure and calcitonin gene-related peptide (CGRP) in response to bacterial and fungal exposures (Baral et al., 2018; Chiu et al., 2013; Cohen et al., 2019; Kashem et al., 2015; Pinho-Ribeiro et al., 2018; Serhan et al., 2019). Papain immunization promoted SP and inhibited CGRP release from skin explants (Figure 5A). This pattern of neuropeptide release was also seen after direct stimulation of DRG cultures with both papain and HDM extract (Figures 5B and S3), indicating that cysteine protease allergens directly stimulate neuropeptide release from sensory neurons. Consistent with this, SP release from skin explants was inhibited by co-injection with QX314 (Figure 5C). In contrast to another report, we found that Alternaria extract, which has serine protease activity, was also capable of inducing DRG release of SP and inhibition of CGRP (Figure S3) (Cayrol et al., 2018; Serhan et al., 2019). These data indicate that the capacity for sensory neuron activation and SP release may be shared among disparate allergens.

We next examined the role of SP in promoting CD301b$^+$ DC migration. The *Tac1* gene encodes for three neuropeptides: SP, Neurokinin A, and Neurokinin K. *Tac1* was not enriched in cutaneous immune cells (Figures S2A and S2B), and despite its role as a pruritogen, *Tac1*$^{-/-}$ mice exhibited intact itch responses to papain (Figure S2D). However, *Tac1*$^{-/-}$ mice did show a decrease in the percent and total number of activated (PDL2$^+$) CD301b$^+$ DCs in the dLN 24 h after papain immunization (Figure 5D). To specifically assess the role of SP and CGRP in CD301b$^+$ DC migration from the skin, we injected photoconverted skin of Kaede mice with OVA and CGRP or SP. Although CGRP had no effect on CD301b$^+$ or CD103$^+$ DC migration, SP injection robustly induced the migration of Kaede^{red} CD301b$^+$ DCs to the dLN (Figures 5E–5G). This SP effect was specific to the migration of Th2 cell skewing CD301b$^+$ DCs; Th1 and Th17 cell-skewing CD103$^+$ dermal DCs were unaffected by SP injection (Figures 5F–5G).

We next examined the role of sensory neurons in CD301b$^+$ DC migration using a patch application model of epicutaneous allergen administration (Figure S4A) (Deckers et al., 2017; Iida et al., 2014). Papain induced robust CD301b$^+$ DC migration as well as a trend for increased SP release from skin explants 24 h after patch placement (Figures S4B–S4D). Application of a single patch led to modest Th2 cell differentiation that was dependent on CD301b$^+$ cells (Figure S4E), underscoring the role for CD301b$^+$ DCs in both i.d. and epicutaneous allergen administration. Despite differences in sensory neuron innervation of epidermis and dermis (Usoskin et al., 2015; Zylka et al., 2005), we found that papain-induced CD301b$^+$ DC migration was significantly decreased in mice depleted of *Trpv1*$^+$ neurons (Figures S4F and S4G). Thus, TRPV1$^+$ neurons act as global regulator of allergen-induced CD301b$^+$ DC migration.

Allergen-Induced Substance P Release and CD301b$^+$ DC Migration Is Mast Cell-Independent

Bidirectional interactions between mast cells and DCs promote both of their functions. Mast cells promote the migration of

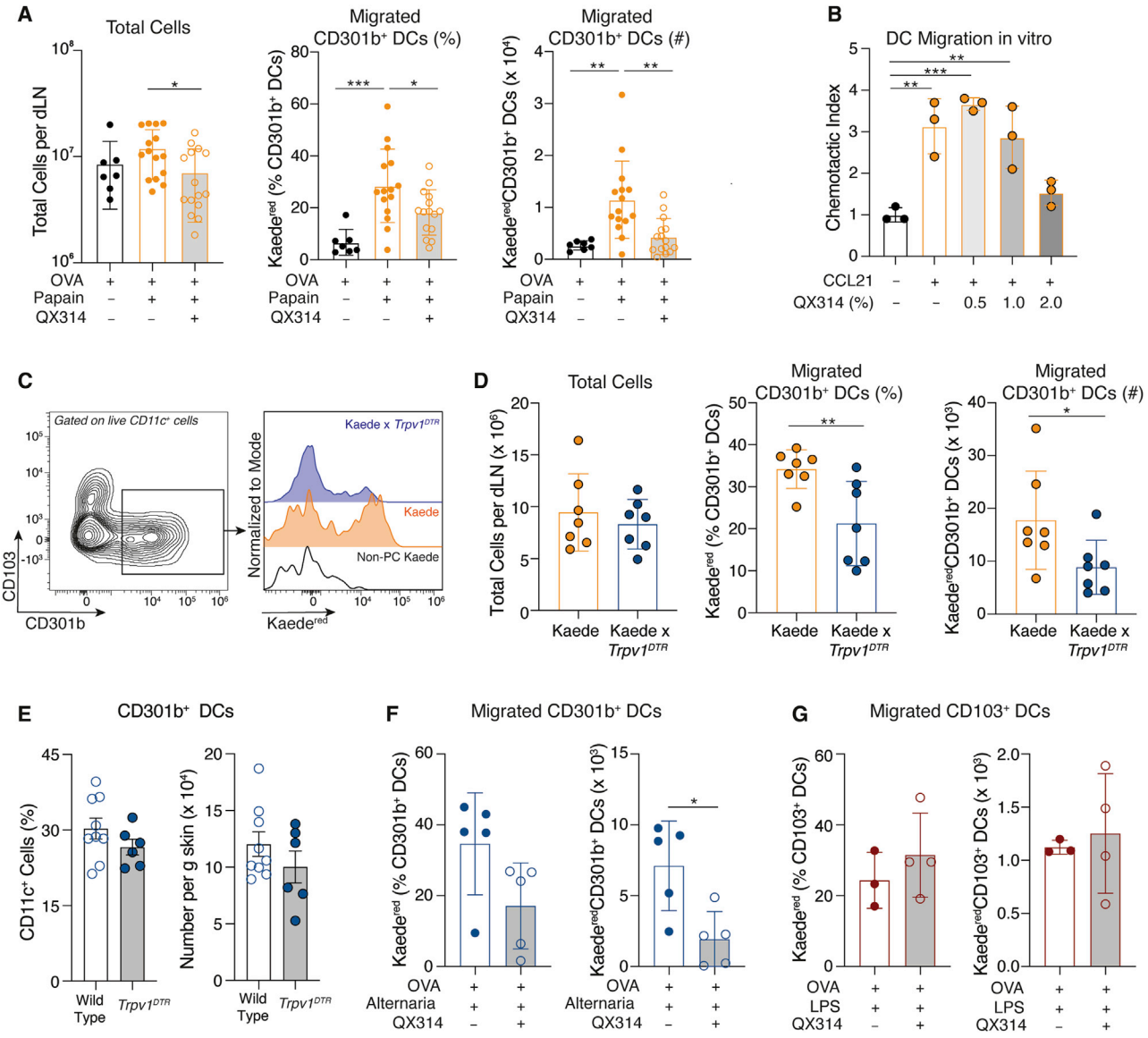

Figure 4. Allergen-Induced Migration of Cutaneous Th2 Cell Skewing CD301b$^+$ Dendritic Cells into the Draining Lymph Node Requires TRPV1$^+$ Sensory Neurons

(A) Total cells per dLN, and percent and number of CD11c$^+$CD301b$^+$ cells (CD301b$^+$ DCs) that migrated from the skin of photoconverted (PC) Kaede transgenic mice (Kaede^{red}) to the dLN 24 h post i.d. injection as indicated.

(B) Transwell migration of BMDCs stimulated overnight with LPS to CCL21 in the presence of 0.5%, 1%, or 2% QX314.

(C) Flow cytometry of CD301b$^+$ DCs from the dLN of DT-treated Kaede or Kaede × *Trpv1*^{DTR} mice 24 h after PC and i.d. immunization with papain.

(D) Total cells per dLN and percent and number of Kaede^{red}CD301b$^+$ DCs was quantified by flow cytometry from mice treated as in (C).

(E) Percent or number per gram (g) skin of CD45$^+$CD11c$^+$MHCII$^+$CD301b$^+$ DCs in DT-treated WT or *Trpv1*^{DTR} mice.

(F and G) Photoconverted Kaede mice were immunized with (F) OVA and Alternaria extract or (G) OVA and LPS in the presence or absence of 1% QX314. The percent and total number of Kaede^{red} (F) CD301b$^+$ DCs or (G) CD103$^+$ DCs were quantified by flow cytometry. Symbols represent individual mice (A and D–G) or replicates (B). Bars indicate mean and error bars indicate SEM. Statistical tests: ordinary one-way ANOVA with multiple comparisons (A and B), unpaired t test (D–G). *p < 0.05, **p < 0.01, ***p < 0.001, ****p < 0.0001. Data are representative of at least three (A–D) or two (E–G) independent experiments, combined in (A), (D), and (E) with each experiment including 2–5 (A and D) or 5–9 (E) mice per group.

See also Figure S2.

DCs to the dLN (Dawicki et al., 2010; Mazzoni et al., 2006; Serhan et al., 2019; Shelburne et al., 2009). Conversely, DCs can transfer antigens to mast cells, thereby promoting their degranulation (Choi et al., 2018). To investigate whether mast cells were involved in our model, we injected papain i.d. in wild-type or mast cell-deficient *Kit*$^{W\text{-}sh/W\text{-}sh}$ mice. c-Kit is expressed by nociceptive neurons and signaling through c-Kit has been shown to prime some TRPV1-mediated responses in nociceptive neurons (Hirata et al., 1993; Milenkovic et al., 2007; Takagi et al., 2008). Thus, any loss of response in Kit mutant mice would be difficult

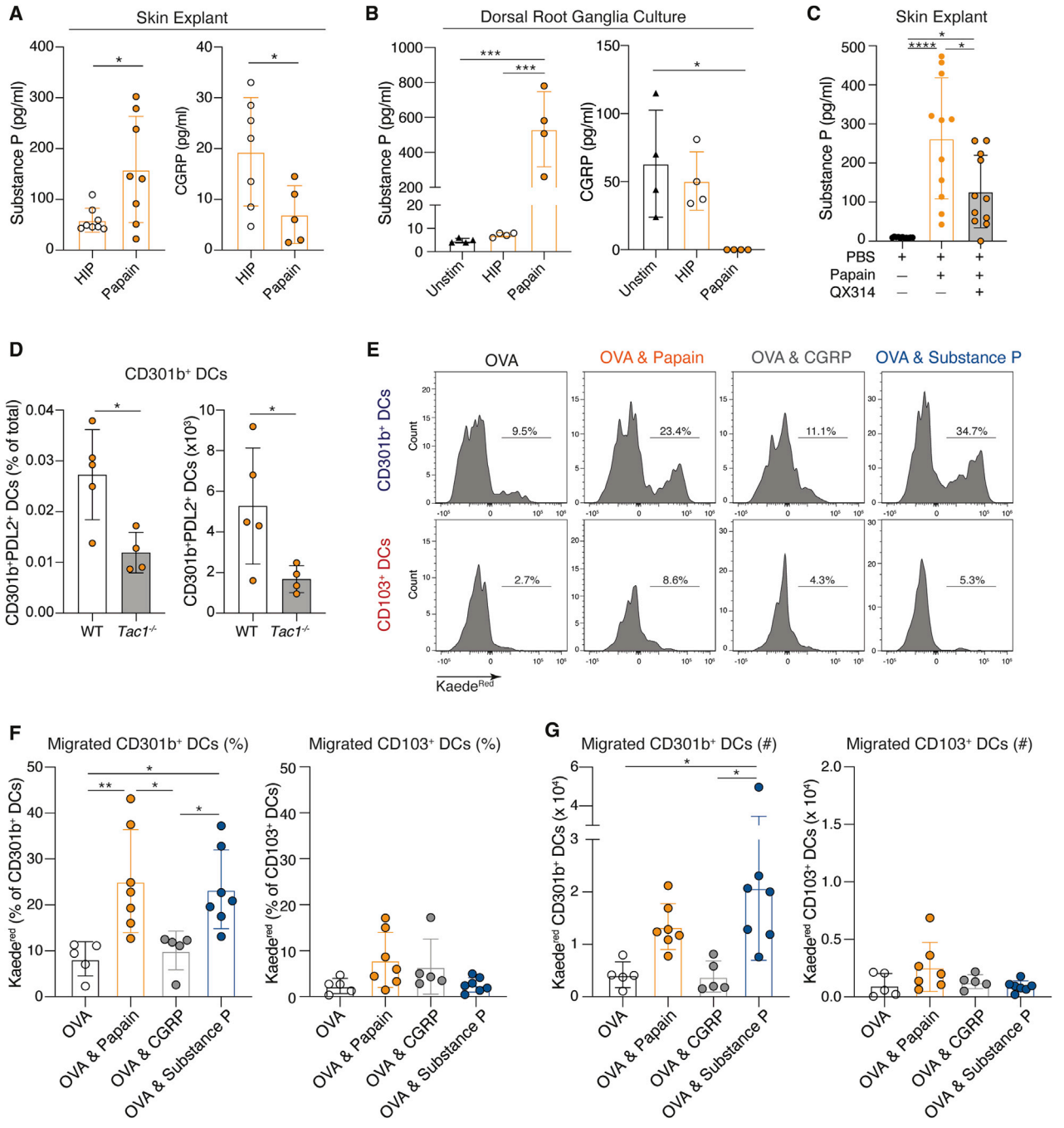

Figure 5. Allergen-Stimulated Sensory Neurons Release Substance P that Induces the Specific Migration of Th2 Cell-Skewing CD301b⁺ Dendritic Cells into the Draining Lymph Node

(A) ELISA for SP and CGRP of skin explant supernatants from WT mice i.d. injected as indicated.

(B) Cultured WT DRG were stimulated as indicated and supernatant was assayed as in (A).

(C) SP release from skin explants of WT mice i.d. injected as indicated.

(D) Percent and number of PDL2⁺CD301b⁺ DCs per dLN of WT or *Tac1*$^{-/-}$ mice 24 h after i.d. immunization with OVA and papain.

(E–G) Flow cytometry of Kaede^{red} live CD11c⁺CD301b⁺ DCs or CD11c⁺CD103⁺ DCs 24 h after photoconversion and the indicated immunization, shown as histograms (E), percent (F), or total number (G). Symbols represent individual mice (A, C, D, F, and G) or replicates (B). Bars indicate mean, and error bars indicate SEM. Statistical tests: unpaired t test (A and D), ordinary one-way ANOVA with multiple comparisons (B, C, F, and G). *p < 0.05, **p < 0.01, ***p < 0.001. Data are representative of at least three independent experiments (B and D), combined in (A, C, F, and G), with each experiment including 2–4 mice per group.

See also Figures S3, S4, and S5.

to assign to their mast cell deficiency or sensory neuron defects. However, we found that the sensory response to papain was unaffected in $Kit^{W\text{-}sh/W\text{-}sh}$ mice (Figure S5A). Despite a role for mast cells and sensory neurons in promoting each other's responses (Azimi et al., 2017; Green et al., 2019; Meixiong et al., 2019a; Serhan et al., 2019), we found no effect of mast cell deficiency on papain-induced SP release from skin explants or DRG cultures (Figures S5B and S5C). Similarly, we found no difference in the percentage or number of activated ($PDL2^+$) $CD301b^+$ DCs in the dLN 24 h after papain-immunization in wild-type or $Kit^{W\text{-}sh/W\text{-}sh}$ mice (Figure S5D). These data indicate that *Kit*-independent neuronal activation, but not mast cell activation, is required for SP release and $CD301b^+$ DC migration.

Substance P Acts through MRGPRA1 on $CD301b^+$ DCs to Promote Their Migration

SP is a cationic neuropeptide that binds to its classical receptors TACR1 and TACR2 as well as the Mas-related G protein coupled receptors MRGPRA1 and MRGPRB2 in the mouse (Azimi et al., 2016, 2017; McNeil et al., 2015). Using the Immgen database we found low, but detectable, expression of *Tacr1* and *Tacr2* in all cutaneous DC subsets and no detectable expression of *Mrgprb2* (Figure S6A). *Mrgpra1* transcript could be detected in the $Langerin^-CD103^-CD11b^+$ DC subset, which contains the dermal $CD301b^+$ DCs (Figure S6A). To confirm these findings, we performed qPCR of bulk BMDCs, which are largely composed of the cDC2s (Gao et al., 2013). BMDCs expressed *Mrgpra1*, but not other known receptors for SP (Figure 6A). To verify this expression on *in vivo* $CD301b^+$ DCs, we sorted $CD301b^+$ DCs and $CD103^+$ DCs from the dLN after papain immunization. We could not reliably detect *Tacr1* or *Tacr2* on either DC subset (Figure S6B). However, $CD301b^+$ DCs, but not $CD103^+$ DCs, expressed *Mrgpra1* indicating that $CD301b^+$ DCs may be specifically sensitive to the effects of SP (Figure 6B). In order to determine the role of MRGRPA1, we sought to block its function using chemical antagonists. Specific antagonists of MRGPRA1 have not been described, so to determine the effects of MRGPRA1 blockade, we compared the effect of the peptide antagonist QWF that blocks TACR1, TACR2, MRGPRB2, and MRGPRA1 to the small molecular antagonist L733060 that only blocks TACR1, TACR2, and MRGPRB2 (Azimi et al., 2016, 2017). Consistent with a role for MRGPRA1 in $CD301b^+$ DC migration, co-immunization with QWF, but not L733060, led to a defect in papain-induced $CD301b^+$ DC migration (Figure 6C).

To this point, our data suggested that SP acts through MRGPRA1, expressed on $CD301b^+$ DCs, to promote the allergen-induced migration of $CD301b^+$ DCs. This effect appeared to be independent of SP-induced CCR7 upregulation (Figure 6D), but to confirm the role of *Mrgpra1* in allergen-induced $CD301b^+$ DC migration *in vivo*, we generated mixed BM chimeras. We transferred an equal ratio of wild-type and $Cd301b^{DTR}$ or $Mrgpra1^{-/-}$ and $Cd301b^{DTR}$ BM into lethally irradiated wild-type recipients to generate $CD301b^{WT}$ and $CD301b^{Mrgpra1-/-}$ chimeras, respectively (Figure 6E). After reconstitution, both groups were treated with DT to yield mice with wild-type sensory neurons, mixed $CD45^+$ immune cell compartments, and either *Mrgpra1*-sufficient ($CD301b^{WT}$) or -deficient ($CD301b^{Mrgpra1-/-}$) $CD301b^+$ DCs (Figure 6E). Consistent with a requirement for *Mrgpra1* in allergen-induced $CD301b^+$ DC migration, papain-induced $CD301b^+$ DC migration was lost in $CD301b^{Mrgpra1-/-}$ chimeras (Figure 6F). In order to directly compare the migration of *Mrgpra1*-sufficient or -deficient $CD301b^+$ DCs *in vivo*, we made additional chimeras in which lethally irradiated wild-type mice were reconstituted with an equal ratio of $CD45.1^+$ wild-type BM and $CD45.2^+$ $Mrgpra1^{-/-}$ BM. We compared the ratio of wild-type versus $Mrgpra1^{-/-}$ $CD301b^+$ DCs in the naive skin to that in the dLN after papain immunization and found that wild-type DCs displayed a significant advantage in allergen-induced migration to the dLN (Figure 6G). This wild-type advantage was lost when examining $CD103^+$ DC migration in response to LPS immunization (Figure 6H), indicating that *Mrgpra1* plays a crucial role in the allergen-induced migration of $CD301b^+$ DCs.

$CD301b^+$ DCs require CCR7 to enter the draining lymphatics and then CCR7 and CCR8 to cross the subcapsular sinus and enter the dLN parenchyma (Sokol et al., 2018). Because $CD301b^+$ DCs do not upregulate CCR7 expression upon allergen immunization, it has remained unclear how $CD301b^+$ DCs are signaled to leave the skin parenchyma to migrate to the draining lymphatic vessels (Sokol et al., 2018). Stimulation with SP or the MRGPRA1 agonist FMRF induced BMDC chemokinesis across a Transwell membrane in the absence of any chemokine gradient (Figure 6I) (Liu et al., 2009). Furthermore, BMDCs stimulated with SP or FMRF exhibited augmented migration to the CCR7 ligand CCL21 (Figure 6J). The effect of SP on chemokinesis and chemotaxis was lost in BMDCs from $Mrgpra1^{-/-}$ mice, indicating that SP promotes DC migration through MRGPRA1 (Figures 6K and 6L) (Meixiong et al., 2019b).

$TRPV1^+$ Neurons Are Required for Th2 Cell Differentiation in Response to Papain

$CD301b^+$ DCs are necessary for Th2 cell differentiation in response to cutaneous allergens, and disruption of their migration into the parenchyma of the dLN blocks Th2 cell differentiation in response to papain (Kumamoto et al., 2013; Sokol et al., 2018). Consistent with their role in allergen-induced $CD301b^+$ DC migration, we found that depletion of $TRPV1^+$ neurons led to decreased allergen-induced Th2 cell differentiation (Figures 7A and 7B). $CD4^+$ T cells expressed significantly less IL-4 (Figure 7C) and IL-13 (Figure 7D), indicating a block in Th2 cell differentiation. There was no concurrent increase in interferon (IFN)γ production by $CD4^+$ T cells, suggesting that this block was related to $CD4^+$ T cell activation and not Th2 cell polarization (Figure 7E). Consistent with this, we found a decrease in the percentage of activated $CD44^{high}$ $CD4^+$ T cells in mice depleted of $TRPV1^+$ neurons (Figure 7F). Similarly, using IL-4-eGFP mice (4get), we found that co-immunization of OVA and papain, together with QX314 or QWF, inhibited the production of IL-4-$eGFP^+$ and activated $CD44^{high}$ and $CD69^{high}$ $CD4^+$ cells as compared to OVA and papain alone (Figures 7G and 7H) (Mohrs et al., 2001). These data suggest that blocking the allergen-induced and *Trpv1*-dependent migration of $CD301b^+$ DCs leads to defective $CD4^+$ T cell activation and Th2 cell differentiation that is secondary to decreased lymph node entry of $CD301b^+$ DCs. Finally, although SP-induced DC migration was necessary for Th2 cell differentiation, it was not sufficient, indicating that an additional signal or cell is required to promote Th2 cell differentiation *in vivo* (Figure 7G).

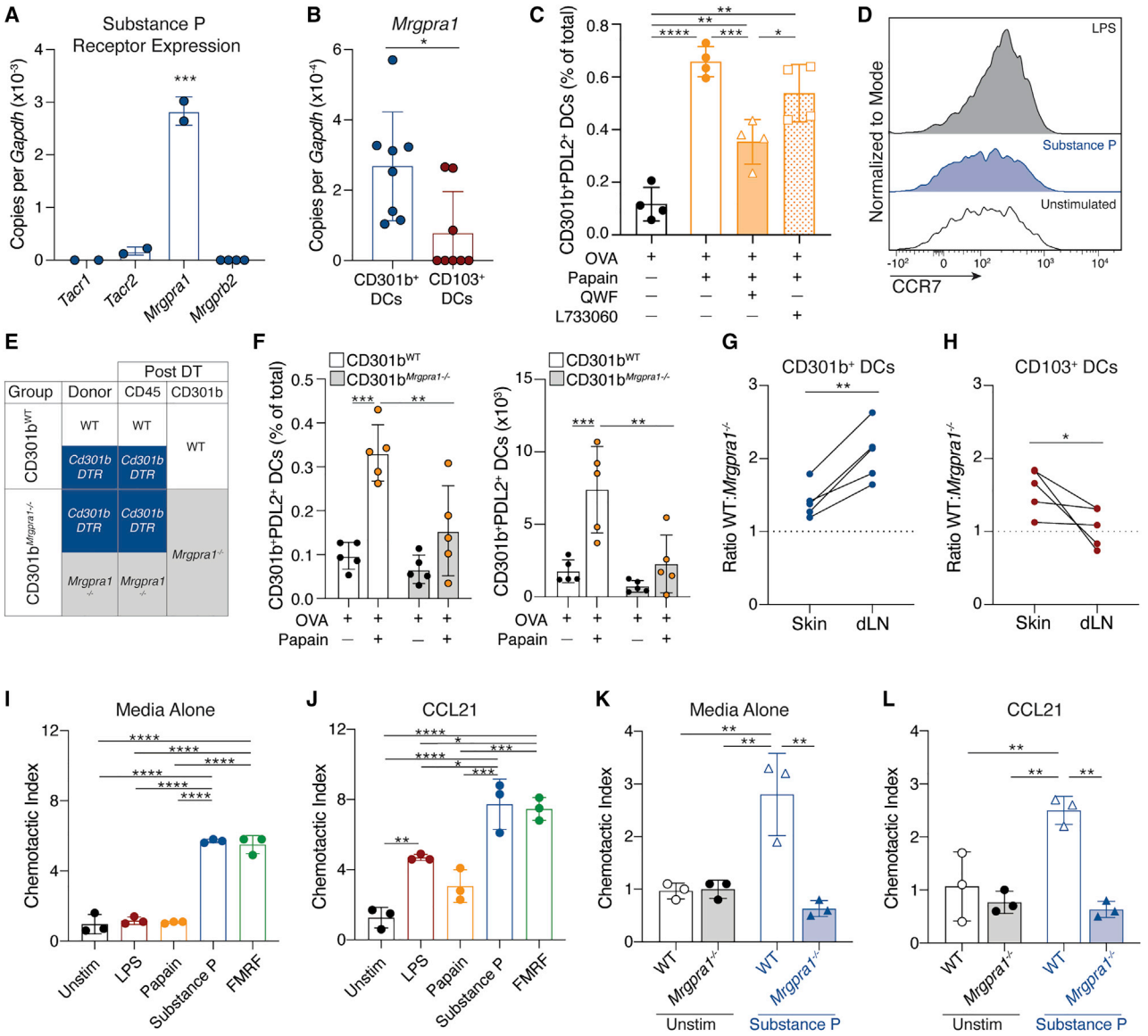

Figure 6. Substance P Promotes Th2 Cell-Skewing CD301b$^+$ Dendritic Cell Migration through Its Receptor *Mrgpra1*

(A) QPCR analysis of *Tacr1*, *Tacr2*, *Mrgpra1*, and *Mrgprb2* from unstimulated BMDCs.

(B) QPCR analysis of *Mrpgra1* expression on live CD11c$^+$CD301b$^+$ (CD301b$^+$ DCs) or CD11c$^+$CD103$^+$ (CD103$^+$ DCs) cells flow sorted from the dLN of WT mice immunized i.d. with papain.

(C) CD301b$^+$PDL2$^+$ DCs in the dLN 24 h after the indicated immunizations.

(D) CCR7 expression by flow cytometry of unstimulated (white), SP stimulated (blue), or LPS stimulated (black) CD11c$^+$CD301b$^+$.

(E) Generation of BM chimeras for comparative migration.

(F) BM chimeras in (E) were treated with DT, immunized as indicated, and the percentage and absolute number of PDL2$^+$ CD301b$^+$ DCs in dLNs were calculated.

(G and H) Mixed BM chimeras of equal ratios of CD45.1$^+$ WT and CD45.2$^+$ *Mrgpra1*$^{-/-}$ BM into lethally irradiated WT recipients were generated. Ratios of WT over *Mrgpra1*$^{-/-}$ (G) CD11c$^+$CD301b$^+$ or (H) CD11c$^+$CD103$^+$ cells from naive ear skin and the dLN 24 h after i.d. (G) papain or (H) LPS immunization of the footpad. Data normalized to total CD45$^+$ cells.

(I and J) WT BMDCs were stimulated overnight as indicated. Transwell migration to media alone (I) or CCL21 (J), normalized to unstimulated BMDCs (chemotactic index).

(K and L) Transwell migration of unstimulated or SP stimulated WT or *Mrgra1*$^{-/-}$ BMDCs as in (I) and (J). Symbols represent individual replicates (A, B, and I–L) or mice (C and F–H), with each mouse serving as its own control in (F)–(H). Histograms are representative individual samples (D). Bars indicate mean and error bars indicate SEM. Statistical tests: ordinary one-way ANOVA with multiple comparisons (A, C, F, and I–L), unpaired t test (B), paired t test (G and H). *p < 0.05, **p < 0.01, ***p < 0.001, ****p < 0.0001. Data are representative of at least two independent experiments, combined in (B), (C), and (H) with each experiment including 2–5 mice per group.

See also Figure S6.

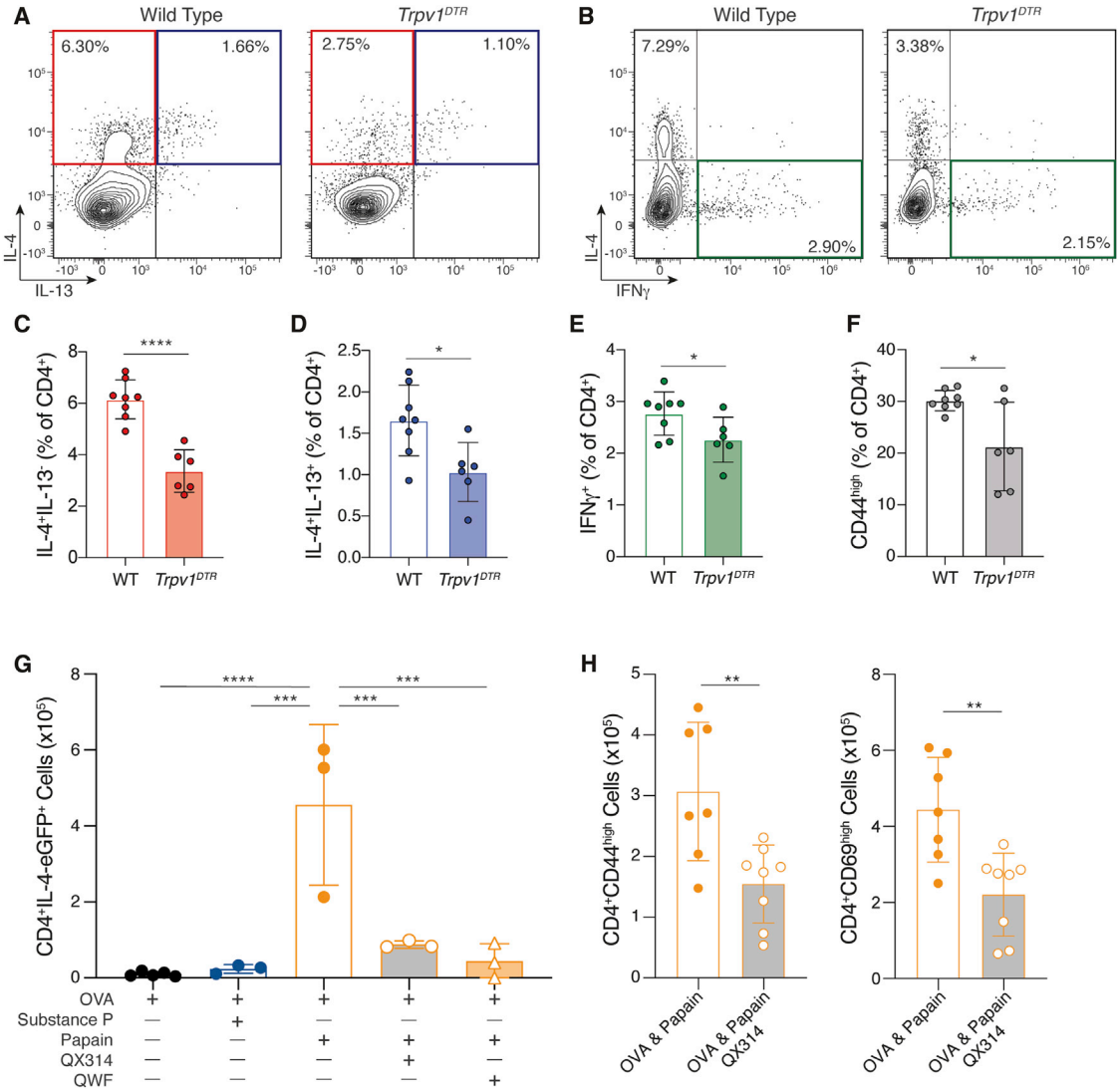

Figure 7. TRPV1$^+$ Neurons Are Required for Th2 Cell Differentiation in Response to the Protease Allergen Papain

(A and B) DT-treated WT or *Trpv1^{DTR}* mice were immunized with OVA and papain. Five days later, flow cytometry was performed for IL-4 and IL-13 (A) or IFNγ (B).

(C–F) Percent of CD4$^+$ cells gated as in (A) and (B) or (F) CD44^{high}.

(G) CD4$^+$IL-4-eGFP$^+$ cells from the dLN of 4get (*IL-4^{eGFP}*) mice 4 days after the indicated immunizations.

(H) CD4$^+$ CD44^{high} or CD69^{high} cells in the dLN 5 days after the indicated immunization. Symbols represent individual mice (C–F). Bars indicate mean and error bars indicate SEM. Statistical tests: ordinary one-way ANOVA with multiple comparisons (G), unpaired t test (C–F and H). *$p < 0.05$, **$p < 0.01$, ***$p < 0.001$, ****$p < 0.0001$. Data are representative of at least two independent experiments, with each experiment including 2–5 mice per group.

DISCUSSION

In the classical PAMP-PRR signaling paradigm, tissue DCs act as direct sensors of type-1 immunogens, such as bacteria and viruses, to initiate adaptive immune responses (Iwasaki and Medzhitov, 2015). Here, we have shown that this paradigm may not be applicable to type-2 (allergic) immunity. We found that TRPV1$^+$ neurons acted as the primary allergen sensor, eliciting the sensation of itch and pain and the release of SP upon exposure. SP then stimulates proximally located Th2 cell-skewing CD301b$^+$ DCs through MRGPRA1 to promote their movement. Activation of sensory neurons was necessary for the initiation of Th2 cell differentiation. We propose that DCs do not directly sense allergens and instead require the initial activation of a primary sensor. In the case of proteolytically active allergens such as papain, HDM, or Alternaria, the sensory nervous system acts as that primary sensor of allergen exposure to initiate the adaptive type-2 immune response. IL-4 and IL-13, produced in the context of chronic allergic inflammation, can decrease the activation threshold of itch sensing neurons, which could link allergen-induced acute activation of the sensory nervous system with chronic allergic inflammation (Oetjen et al., 2017).

Our study revealed that SP acts through MRGPRA1 to induce the migration of CD301b$^+$ DCs to the dLN. Importantly, SP-induced migration was not sufficient for Th2 cell differentiation. This is consistent with studies showing an important role for

innate alarmins in Th2 cell differentiation and allergic inflammation, but only a partial role in DC migration (Besnard et al., 2011; Cayrol et al., 2018; Palm et al., 2013). Both signals may be required to fully license the DC to promote Th2 cell differentiation, or they may individually act on DCs and putative accessory cells that provide the necessary skewing information for Th2 cell differentiation (Halim et al., 2018). This two-signal requirement could be essential to reduce the risk of non-specific or bystander activation of DCs. Unlike PAMPs, which DCs normally interact with in the context of antigens, indirect activation of DCs by neurons separates the activation trigger from the antigen. If both sensory neuron activation and alarmins are required for full DC licensing, this may limit DC activation to those DCs in areas of high antigen concentration. However, this separation of antigen from adjuvant detection runs the risk of activating DCs presenting bystander antigens and could underlie the clinical observation of ''allergen creep'' in which atopic individuals progressively gain additional allergen sensitizations (Brough et al., 2015; Migueres et al., 2014).

Why is SP required for DC migration in the type-2 immune response? Unlike in the PAMP-PRR signaling paradigm, DCs fail to directly sense allergen-associated molecular patterns and do not upregulate CCR7 upon allergen exposure. We propose that the SP signal is necessary to induce chemokinesis, allowing Th2 cell skewing CD301b$^+$ DCs to release contacts from within the dermis. How SP induces chemokinesis is unknown, but it is possible that MRGRPA1 signaling promotes Src phosphorylation, which we and others have shown to be necessary for optimal DC migration (Hauser et al., 2016; Sokol et al., 2018). Unanchored CD301b$^+$ DCs can then utilize their baseline expression of CCR7, which is necessary for their migration into draining lymphatics, to sense and respond to homeostatic CCL21 gradients and migrate to the dLN (Ohl et al., 2004; Sokol et al., 2018). This provides a potential mechanism by which allergen-activated DCs—in contrast to mast cells that can directly respond to allergens through IgE cross-linking—are able to sense and migrate out of the peripheral tissues without direct allergen detection and without concomitant upregulation of CCR7 (Lin et al., 2018). It also raises an important question as to why cDC2s are specifically required for Th2 cell differentiation. cDC2s may provide unique Th2 cell skewing signals in the dLN or they may act upon sensory neurons in the skin to promote their activation (Xu et al., 2020). Alternatively, could cDC2s be required for Th2 cell differentiation simply because their expression of *Mrgpra1* endows them with the unique ability to migrate to the dLN in response to allergen exposure? If so, forced expression of *Mrgpra1* on different DC subsets should be sufficient to endow other DCs with Th2 cell skewing capability.

Cysteine protease allergens, including papain and HDM, induce Ca^{2+} flux of DRG neurons in culture that indicates that nociceptive neurons directly sense allergens (Reddy et al., 2015; Serhan et al., 2019). How this sensing occurs is unclear. Protease activated receptors (PARs) 2 and 4 are cleaved by papain and have been associated with the itch response, but the interpretation of some of these studies is complicated by the fact that the PAR2 agonist SLIGRL also activates MRGPRC11 to mediate itch (Liu et al., 2011). Indeed, the MRGPR family plays a major role in neuronal itch sensing, with MRGPRA3 mediating chloroquine-induced itch and MRGPRA1 mediating bilirubin-induced itch (Liu et al., 2009; Meixiong et al., 2019b). MRGPRs are expressed on both mast cells and sensory neurons, permitting these cells to directly communicate through the release of preformed mediators including neuropeptides to promote itch and allergic inflammation (Meixiong et al., 2019a; Serhan et al., 2019). Here, we found that CD301b$^+$ DCs expressed MRGPRA1, but not other SP receptors. This may permit CD301b$^+$ DC migration to be directly activated by MRGPRA1 agonists, such as bilirubin (Meixiong et al., 2019b). We found that CD301b$^+$ DC expression of MRGPRA1 allowed them to sense SP from sensory neurons and migrate in response to allergen exposure, although this data from mixed BM chimeras will ultimately need to be confirmed using a model in which *Mrgpra1* is specifically ablated in CD301b$^+$ DCs. Our data are in contrast to reports showing that various DC subsets express *Tacr1* and respond to SP and its analogs by promoting DC survival and migration, as well as skewed Th1 cell and cytotoxic T cell responses (Janelsins et al., 2009, 2013; Mathers et al., 2007). We did not detect *Tacr1* in CD301b$^+$ DCs, but it is possible that differential expression of SP receptors by DC subsets could lead to different functional outcomes. Ultimately, this communication between the sensory nervous system and immune cells could be a rapid way to initiate protective host defenses (Cohen et al., 2019; Kashem et al., 2015), but its dysregulation could drive inflammatory or allergic diseases (Riol-Blanco et al., 2014; Talbot et al., 2015; Tränkner et al., 2014).

The critical role of TRPV1$^+$ sensory neurons and SP-driven DC migration in the development of allergic immune responses to cutaneous allergens provides a targetable pathway for the prevention and treatment of allergic diseases. TRPV1$^+$ neurons activated optogenetically or by *Candida* infection release CGRP that promotes activation of the IL-17-mediated anti-fungal immune response (Cohen et al., 2019; Kashem et al., 2015). How *Candida* can promote CGRP release while protease allergens induce SP release is unclear. Although *Candida* and protease allergens may activate different subsets of TRPV1$^+$ neurons, TRPV1$^+$ neurons may also be able to differentiate between stimuli to promote different immune responses through unique neuropeptide release patterns. CGRP release may specifically induce innate IL-17-related inflammatory responses, whereas SP may specifically induce initiation of the type-2 adaptive immune response. SP has already been shown to directly activate mast cells through MRGPRB2 (Serhan et al., 2019), could SP act as a master regulator of innate type-2 immune cells? The full extent of how CGRP and SP specifically activate different arms of Th-mediated immunity remain unclear, however, exploiting the neuropeptide specificity for initiating type-1, type-2, and type-17 immune responses would allow for targeted therapeutics. The TACR1 antagonist serlopitant has recently been shown to be effective in the treatment of chronic itch (Yosipovitch et al., 2018). Although our data suggest that TACR1 antagonists are unlikely to alter CD301b$^+$ DC migration, drugs that target MRGPRX2, the human ortholog of MRGPRA1, may be targets for allergic diseases. Conversely, many common drugs act as MRGPRX2 agonists (McNeil et al., 2015). Whether this leads to DC migration and allergic sensitization in humans remains unknown. Together, these data establish mechanisms for DC migration in allergic immune responses that may be applied to the prevention and treatment of allergic diseases.

STAR★METHODS

Detailed methods are provided in the online version of this paper and include the following:

- KEY RESOURCES TABLE
- RESOURCE AVAILABILITY
  - Lead Contact
  - Materials Availability
  - Data and Code Availability
- EXPERIMENTAL MODEL AND SUBJECT DETAILS
  - Mice
  - Experimental Mouse Models
  - Kaede Photoconversion
  - Bone Marrow Chimera Generation
  - Cell or Tissue Isolation and Culture
  - Dorsal Root Ganglia Cultures and Stimulation
  - Flank Explant Assay
  - Generation of Bone Marrow-derived Dendritic Cells (BMDCs)
  - Stimulation of Primary Dendritic Cells
- METHOD DETAILS
  - Intradermal Immunizations
  - Epicutaneous Sensitization
  - Behavioral Analysis
  - Calcium Imaging of DRG Neuronal Cultures
  - Microscopy and Image Quantification
  - Enzyme-Linked Immunosorbent Assay (ELISA)
  - Flow Cytometry and Cell Sorting
  - Quantitative PCR (qPCR)
  - Chemotaxis Assays
- QUANTIFICATION AND STATISTICAL ANALYSIS

SUPPLEMENTAL INFORMATION

Supplemental Information can be found online at https://doi.org/10.1016/j.immuni.2020.10.001.

ACKNOWLEDGMENTS

We thank N. Andrew (MGH) for technical advice, M. Hoon (NIH) for providing *Trpv1*^{DTR} mice, K. Blake and S. Sannajust (Harvard) for breeding *Tac1*$^{-/-}$, *Nav1.8*^{cre}, and *tdTomato*^{loxSTOPlox} mice, and X. Dong (Johns Hopkins) for providing *Mrgpra1*$^{-/-}$ bone marrow. BioRender.com was used to produce the graphical abstract. Cytometric findings reported here were performed in the MGH Department of Pathology Flow and Image Cytometry Research Core, with support from the NIH Shared Instrumentation Program (1S10OD012027-01A1, 1S10OD016372-01, 1S10RR020936-01, and 1S10RR023440-01A1). This work was supported by NIH K08AI121421 (to C.L.S), DP2AT009499 and R01AI130019 (to I.M.C.), T32HL116275 (to C.H.F.), DFG PE2864/3-1 (to C.P.), Center for the Study of Inflammatory Bowel Disease Pilot Feasibility Study Award (DK043351 to C.L.S.), Massachusetts General Hospital Transformative Scholar Award (to C.L.S.), AAAAI Foundation and Dr. Donald Y. M. Leung/JACI Editors Faculty Development Award (to C.L.S.), and Food Allergy Science Initiative (to C.L.S. and I.M.C.). I.M.C. receives additional support from the Chan Zuckerberg Initiative, Burroughs Wellcome Fund, Harvard Stem Cell Institute, GlaxoSmithKline (GSK), and Allergan Pharmaceuticals.

AUTHOR CONTRIBUTIONS

C.P., C.H.F., X.Z., P.A.A., Z.N.A.D., and C.L.S. designed the study. C.P., C.H.F., X.Z., P.A.A., Z.N.A.D., T.V., R.B.C., O.A.C., and C.L.S. performed and/or analyzed experiments. C.P., C.H.F., P.A.A., Z.N.A.D., and C.L.S. wrote the manuscript. I.M.C. provided resources and advice. C.L.S. provided resources, reagents, and funding. C.L.S. supervised the study.

DECLARATION OF INTERESTS

C.L.S. is a paid consultant for Bayer and Merck. P.A.A. is a current employee of Skyhawk Therapeutics. I.M.C. receives sponsored research support from GSK and Allergan Pharmaceuticals. I.M.C. is on the scientific advisory boards of GSK and Kintai Pharmaceuticals.

Received: April 2, 2020
Revised: July 21, 2020
Accepted: September 30, 2020
Published: October 23, 2020

REFERENCES

Abrahamsen, B., Zhao, J., Asante, C.O., Cendan, C.M., Marsh, S., Martinez-Barbera, J.P., Nassar, M.A., Dickenson, A.H., and Wood, J.N. (2008). The cell and molecular basis of mechanical, cold, and inflammatory pain. Science *321*, 702–705.

Azimi, E., Reddy, V.B., Pereira, P.J.S., Talbot, S., Woolf, C.J., and Lerner, E.A. (2017). Substance P activates Mas-related G protein-coupled receptors to induce itch. J. Allergy Clin. Immunol. *140*, 447–453.

Azimi, E., Reddy, V.B., Shade, K.C., Anthony, R.M., Talbot, S., Pereira, P.J.S., and Lerner, E.A. (2016). Dual action of neurokinin-1 antagonists on Mas-related GPCRs. JCI Insight *1*, e89362.

Baral, P., Umans, B.D., Li, L., Wallrapp, A., Bist, M., Kirschbaum, T., Wei, Y., Zhou, Y., Kuchroo, V.K., Burkett, P.R., et al. (2018). Nociceptor sensory neurons suppress neutrophil and γδ T cell responses in bacterial lung infections and lethal pneumonia. Nat. Med. *24*, 417–426.

Besnard, A.G., Togbe, D., Guillou, N., Erard, F., Quesniaux, V., and Ryffel, B. (2011). IL-33-activated dendritic cells are critical for allergic airway inflammation. Eur. J. Immunol. *41*, 1675–1686.

Binshtok, A.M., Bean, B.P., and Woolf, C.J. (2007). Inhibition of nociceptors by TRPV1-mediated entry of impermeant sodium channel blockers. Nature *449*, 607–610.

Brough, H.A., Liu, A.H., Sicherer, S., Makinson, K., Douiri, A., Brown, S.J., Stephens, A.C., Irwin McLean, W.H., Turcanu, V., Wood, R.A., et al. (2015). Atopic dermatitis increases the effect of exposure to peanut antigen in dust on peanut sensitization and likely peanut allergy. J. Allergy Clin. Immunol. *135*, 164–170.

Cayrol, C., Duval, A., Schmitt, P., Roga, S., Camus, M., Stella, A., Burlet-Schiltz, O., Gonzalez-de-Peredo, A., and Girard, J.P. (2018). Environmental allergens induce allergic inflammation through proteolytic maturation of IL-33. Nat. Immunol. *19*, 375–385.

Chen, J., and Lariviere, W.R. (2010). The nociceptive and anti-nociceptive effects of bee venom injection and therapy: a double-edged sword. Prog. Neurobiol. *92*, 151–183.

Chiu, I.M., Heesters, B.A., Ghasemlou, N., Von Hehn, C.A., Zhao, F., Tran, J., Wainger, B., Strominger, A., Muralidharan, S., Horswill, A.R., et al. (2013). Bacteria activate sensory neurons that modulate pain and inflammation. Nature *501*, 52–57.

Choi, H.W., Suwanpradid, J., Kim, I.H., Staats, H.F., Haniffa, M., MacLeod, A.S., and Abraham, S.N. (2018). Perivascular dendritic cells elicit anaphylaxis by relaying allergens to mast cells via microvesicles. Science *362*, eaao0666.

Cohen, J.A., Edwards, T.N., Liu, A.W., Hirai, T., Jones, M.R., Wu, J., Li, Y., Zhang, S., Ho, J., Davis, B.M., et al. (2019). Cutaneous TRPV1(+) Neurons Trigger Protective Innate Type 17 Anticipatory Immunity. Cell *178*, 919–932.

Dawicki, W., Jawdat, D.W., Xu, N., and Marshall, J.S. (2010). Mast cells, histamine, and IL-6 regulate the selective influx of dendritic cell subsets into an inflamed lymph node. J. Immunol. *184*, 2116–2123.

Deckers, J., Sichien, D., Plantinga, M., Van Moorleghem, J., Vanheerswynghels, M., Hoste, E., Malissen, B., Dombrowicz, D., Guilliams,

M., De Bosscher, K., et al. (2017). Epicutaneous sensitization to house dust mite allergen requires interferon regulatory factor 4-dependent dermal dendritic cells. J. Allergy Clin. Immunol. *140*, 1364–1377.

Gao, Y., Nish, S.A., Jiang, R., Hou, L., Licona-Limón, P., Weinstein, J.S., Zhao, H., and Medzhitov, R. (2013). Control of T helper 2 responses by transcription factor IRF4-dependent dendritic cells. Immunity *39*, 722–732.

Green, D.P., Limjunyawong, N., Gour, N., Pundir, P., and Dong, X. (2019). A Mast-Cell-Specific Receptor Mediates Neurogenic Inflammation and Pain. Neuron *101*, 412–420.

Guzmán, M., Miglio, M.S., Zgajnar, N.R., Colado, A., Almejún, M.B., Keitelman, I.A., Sabbione, F., Fuentes, F., Trevani, A.S., Giordano, M.N., and Galletti, J.G. (2018). The mucosal surfaces of both eyes are immunologically linked by a neurogenic inflammatory reflex involving TRPV1 and substance P. Mucosal Immunol. *11*, 1441–1453.

Halim, T.Y., Steer, C.A., Mathä, L., Gold, M.J., Martinez-Gonzalez, I., McNagny, K.M., McKenzie, A.N., and Takei, F. (2014). Group 2 innate lymphoid cells are critical for the initiation of adaptive T helper 2 cell-mediated allergic lung inflammation. Immunity *40*, 425–435.

Halim, T.Y.F., Rana, B.M.J., Walker, J.A., Kerscher, B., Knolle, M.D., Jolin, H.E., Serrao, E.M., Haim-Vilmovsky, L., Teichmann, S.A., Rodewald, H.R., et al. (2018). Tissue-Restricted Adaptive Type 2 Immunity Is Orchestrated by Expression of the Costimulatory Molecule OX40L on Group 2 Innate Lymphoid Cells. Immunity *48*, 1195–1207.

Hauser, M.A., Schaeuble, K., Kindinger, I., Impellizzieri, D., Krueger, W.A., Hauck, C.R., Boyman, O., and Legler, D.F. (2016). Inflammation-Induced CCR7 Oligomers Form Scaffolds to Integrate Distinct Signaling Pathways for Efficient Cell Migration. Immunity *44*, 59–72.

Heng, T.S.P., and Painter, M.W.; Immunological Genome Project Consortium (2008). The Immunological Genome Project: networks of gene expression in immune cells. Nat. Immunol. *9*, 1091–1094.

Hirata, T., Morii, E., Morimoto, M., Kasugai, T., Tsujimura, T., Hirota, S., Kanakura, Y., Nomura, S., and Kitamura, Y. (1993). Stem cell factor induces outgrowth of c-kit-positive neurites and supports the survival of c-kit-positive neurons in dorsal root ganglia of mouse embryos. Development *119*, 49–56.

Hosoi, J., Murphy, G.F., Egan, C.L., Lerner, E.A., Grabbe, S., Asahina, A., and Granstein, R.D. (1993). Regulation of Langerhans cell function by nerves containing calcitonin gene-related peptide. Nature *363*, 159–163.

Iida, H., Takai, T., Hirasawa, Y., Kamijo, S., Shimura, S., Ochi, H., Nishioka, I., Maruyama, N., Ogawa, H., Okumura, K., and Ikeda, S. (2014). Epicutaneous administration of papain induces IgE and IgG responses in a cysteine protease activity-dependent manner. Allergol. Int. *63*, 219–226.

Iwasaki, A., and Medzhitov, R. (2015). Control of adaptive immunity by the innate immune system. Nat. Immunol. *16*, 343–353.

Janelsins, B.M., Mathers, A.R., Tkacheva, O.A., Erdos, G., Shufesky, W.J., Morelli, A.E., and Larregina, A.T. (2009). Proinflammatory tachykinins that signal through the neurokinin 1 receptor promote survival of dendritic cells and potent cellular immunity. Blood *113*, 3017–3026.

Janelsins, B.M., Sumpter, T.L., Tkacheva, O.A., Rojas-Canales, D.M., Erdos, G., Mathers, A.R., Shufesky, W.J., Storkus, W.J., Falo, L.D., Jr., Morelli, A.E., and Larregina, A.T. (2013). Neurokinin-1 receptor agonists bias therapeutic dendritic cells to induce type 1 immunity by licensing host dendritic cells to produce IL-12. Blood *121*, 2923–2933.

Joost, S., Annusver, K., Jacob, T., Sun, X., Dalessandri, T., Sivan, U., Sequeira, I., Sandberg, R., and Kasper, M. (2020). The Molecular Anatomy of Mouse Skin during Hair Growth and Rest. Cell Stem Cell *26*, 441–457.

Kashem, S.W., Riedl, M.S., Yao, C., Honda, C.N., Vulchanova, L., and Kaplan, D.H. (2015). Nociceptive Sensory Fibers Drive Interleukin-23 Production from CD301b+ Dermal Dendritic Cells and Drive Protective Cutaneous Immunity. Immunity *43*, 515–526.

Kumamoto, Y., Linehan, M., Weinstein, J.S., Laidlaw, B.J., Craft, J.E., and Iwasaki, A. (2013). CD301b^{+} dermal dendritic cells drive T helper 2 cell-mediated immunity. Immunity *39*, 733–743.

Lai, N.Y., Musser, M.A., Pinho-Ribeiro, F.A., Baral, P., Jacobson, A., Ma, P., Potts, D.E., Chen, Z., Paik, D., Soualhi, S., et al. (2020). Gut-Innervating Nociceptor Neurons Regulate Peyer's Patch Microfold Cells and SFB Levels to Mediate Salmonella Host Defense. Cell *180*, 33–49.

Lamhamedi-Cherradi, S.E., Martin, R.E., Ito, T., Kheradmand, F., Corry, D.B., Liu, Y.J., and Moyle, M. (2008). Fungal proteases induce Th2 polarization through limited dendritic cell maturation and reduced production of IL-12. J. Immunol. *180*, 6000–6009.

Lin, Y.P., Nelson, C., Kramer, H., and Parekh, A.B. (2018). The Allergen Der p3 from House Dust Mite Stimulates Store-Operated Ca(2+) Channels and Mast Cell Migration through PAR4 Receptors. Mol. Cell *70*, 228–241.

Liu, Q., Tang, Z., Surdenikova, L., Kim, S., Patel, K.N., Kim, A., Ru, F., Guan, Y., Weng, H.J., Geng, Y., et al. (2009). Sensory neuron-specific GPCR Mrgprs are itch receptors mediating chloroquine-induced pruritus. Cell *139*, 1353–1365.

Liu, Q., Weng, H.J., Patel, K.N., Tang, Z., Bai, H., Steinhoff, M., and Dong, X. (2011). The distinct roles of two GPCRs, MrgprC11 and PAR2, in itch and hyperalgesia. Sci. Signal. *4*, ra45.

Liu, Y.J., Soumelis, V., Watanabe, N., Ito, T., Wang, Y.H., Malefyt, Rde.W., Omori, M., Zhou, B., and Ziegler, S.F. (2007). TSLP: an epithelial cell cytokine that regulates T cell differentiation by conditioning dendritic cell maturation. Annu. Rev. Immunol. *25*, 193–219.

Mathers, A.R., Tckacheva, O.A., Janelsins, B.M., Shufesky, W.J., Morelli, A.E., and Larregina, A.T. (2007). In vivo signaling through the neurokinin 1 receptor favors transgene expression by Langerhans cells and promotes the generation of Th1- and Tc1-biased immune responses. J. Immunol. *178*, 7006–7017.

Mazzoni, A., Siraganian, R.P., Leifer, C.A., and Segal, D.M. (2006). Dendritic cell modulation by mast cells controls the Th1/Th2 balance in responding T cells. J. Immunol. *177*, 3577–3581.

McNeil, B.D., Pundir, P., Meeker, S., Han, L., Undem, B.J., Kulka, M., and Dong, X. (2015). Identification of a mast-cell-specific receptor crucial for pseudo-allergic drug reactions. Nature *519*, 237–241.

Meixiong, J., Anderson, M., Limjunyawong, N., Sabbagh, M.F., Hu, E., Mack, M.R., Oetjen, L.K., Wang, F., Kim, B.S., and Dong, X. (2019a). Activation of Mast-Cell-Expressed Mas-Related G-Protein-Coupled Receptors Drives Non-histaminergic Itch. Immunity *50*, 1163–1171.

Meixiong, J., Vasavda, C., Green, D., Zheng, Q., Qi, L., Kwatra, S.G., Hamilton, J.P., Snyder, S.H., and Dong, X. (2019b). Identification of a bilirubin receptor that may mediate a component of cholestatic itch. eLife *8*, e44116.

Migueres, M., Dávila, I., Frati, F., Azpeitia, A., Jeanpetit, Y., Lhéritier-Barrand, M., Incorvaia, C., and Ciprandi, G. (2014). Types of sensitization to aeroallergens: definitions, prevalences and impact on the diagnosis and treatment of allergic respiratory disease. Clin. Transl. Allergy *4*, 16.

Milenkovic, N., Frahm, C., Gassmann, M., Griffel, C., Erdmann, B., Birchmeier, C., Lewin, G.R., and Garratt, A.N. (2007). Nociceptive tuning by stem cell factor/c-Kit signaling. Neuron *56*, 893–906.

Mohrs, M., Shinkai, K., Mohrs, K., and Locksley, R.M. (2001). Analysis of type 2 immunity in vivo with a bicistronic IL-4 reporter. Immunity *15*, 303–311.

Oetjen, L.K., Mack, M.R., Feng, J., Whelan, T.M., Niu, H., Guo, C.J., Chen, S., Trier, A.M., Xu, A.Z., Tripathi, S.V., et al. (2017). Sensory Neurons Co-opt Classical Immune Signaling Pathways to Mediate Chronic Itch. Cell *171*, 217–228.

Ohl, L., Mohaupt, M., Czeloth, N., Hintzen, G., Kiafard, Z., Zwirner, J., Blankenstein, T., Henning, G., and Förster, R. (2004). CCR7 governs skin dendritic cell migration under inflammatory and steady-state conditions. Immunity *21*, 279–288.

Palm, N.W., Rosenstein, R.K., and Medzhitov, R. (2012). Allergic host defences. Nature *484*, 465–472.

Palm, N.W., Rosenstein, R.K., Yu, S., Schenten, D.D., Florsheim, E., and Medzhitov, R. (2013). Bee venom phospholipase A2 induces a primary type 2 response that is dependent on the receptor ST2 and confers protective immunity. Immunity *39*, 976–985.

Pinho-Ribeiro, F.A., Baddal, B., Haarsma, R., O'Seaghdha, M., Yang, N.J., Blake, K.J., Portley, M., Verri, W.A., Dale, J.B., Wessels, M.R., et al. (2018). Blocking Neuronal Signaling to Immune Cells Treats Streptococcal Invasive Infection. Cell *173*, 1083–1097.

Pogorzala, L.A., Mishra, S.K., and Hoon, M.A. (2013). The cellular code for mammalian thermosensation. J. Neurosci. *33*, 5533–5541.

Porter, P., Susarla, S.C., Polikepahad, S., Qian, Y., Hampton, J., Kiss, A., Vaidya, S., Sur, S., Ongeri, V., Yang, T., et al. (2009). Link between allergic asthma and airway mucosal infection suggested by proteinase-secreting household fungi. Mucosal Immunol. *2*, 504–517.

Rank, M.A., Kobayashi, T., Kozaki, H., Bartemes, K.R., Squillace, D.L., and Kita, H. (2009). IL-33-activated dendritic cells induce an atypical TH2-type response. J. Allergy Clin. Immunol. *123*, 1047–1054.

Reddy, V.B., and Lerner, E.A. (2010). Plant cysteine proteases that evoke itch activate protease-activated receptors. Br. J. Dermatol. *163*, 532–535.

Reddy, V.B., Sun, S., Azimi, E., Elmariah, S.B., Dong, X., and Lerner, E.A. (2015). Redefining the concept of protease-activated receptors: cathepsin S evokes itch via activation of Mrgprs. Nat. Commun. *6*, 7864.

Riol-Blanco, L., Ordovas-Montanes, J., Perro, M., Naval, E., Thiriot, A., Alvarez, D., Paust, S., Wood, J.N., and von Andrian, U.H. (2014). Nociceptive sensory neurons drive interleukin-23-mediated psoriasiform skin inflammation. Nature *510*, 157–161.

Roberson, D.P., Gudes, S., Sprague, J.M., Patoski, H.A., Robson, V.K., Blasl, F., Duan, B., Oh, S.B., Bean, B.P., Ma, Q., et al. (2013). Activity-dependent silencing reveals functionally distinct itch-generating sensory neurons. Nat. Neurosci. *16*, 910–918.

Serhan, N., Basso, L., Sibilano, R., Petitfils, C., Meixiong, J., Bonnart, C., Reber, L.L., Marichal, T., Starkl, P., Cenac, N., et al. (2019). House dust mites activate nociceptor-mast cell clusters to drive type 2 skin inflammation. Nat. Immunol. *20*, 1435–1443.

Shelburne, C.P., Nakano, H., St John, A.L., Chan, C., McLachlan, J.B., Gunn, M.D., Staats, H.F., and Abraham, S.N. (2009). Mast cells augment adaptive immunity by orchestrating dendritic cell trafficking through infected tissues. Cell Host Microbe *6*, 331–342.

Sokol, C.L., Barton, G.M., Farr, A.G., and Medzhitov, R. (2008). A mechanism for the initiation of allergen-induced T helper type 2 responses. Nat. Immunol. *9*, 310–318.

Sokol, C.L., Camire, R.B., Jones, M.C., and Luster, A.D. (2018). The Chemokine Receptor CCR8 Promotes the Migration of Dendritic Cells into the Lymph Node Parenchyma to Initiate the Allergic Immune Response. Immunity *49*, 449–463.

Stirling, L.C., Forlani, G., Baker, M.D., Wood, J.N., Matthews, E.A., Dickenson, A.H., and Nassar, M.A. (2005). Nociceptor-specific gene deletion using heterozygous NaV1.8-Cre recombinase mice. Pain *113*, 27–36.

Strid, J., Hourihane, J., Kimber, I., Callard, R., and Strobel, S. (2004). Disruption of the stratum corneum allows potent epicutaneous immunization with protein antigens resulting in a dominant systemic Th2 response. Eur. J. Immunol. *34*, 2100–2109.

Takagi, K., Okuda-Ashitaka, E., Mabuchi, T., Katano, T., Ohnishi, T., Matsumura, S., Ohnaka, M., Kaneko, S., Abe, T., Hirata, T., et al. (2008). Involvement of stem cell factor and its receptor tyrosine kinase c-kit in pain regulation. Neuroscience *153*, 1278–1288.

Talbot, S., Abdulnour, R.E., Burkett, P.R., Lee, S., Cronin, S.J., Pascal, M.A., Laedermann, C., Foster, S.L., Tran, J.V., Lai, N., et al. (2015). Silencing Nociceptor Neurons Reduces Allergic Airway Inflammation. Neuron *87*, 341–354.

Talbot, S., Foster, S.L., and Woolf, C.J. (2016). Neuroimmunity: Physiology and Pathology. Annu. Rev. Immunol. *34*, 421–447.

Tang, H., Cao, W., Kasturi, S.P., Ravindran, R., Nakaya, H.I., Kundu, K., Murthy, N., Kepler, T.B., Malissen, B., and Pulendran, B. (2010). The T helper type 2 response to cysteine proteases requires dendritic cell-basophil cooperation via ROS-mediated signaling. Nat. Immunol. *11*, 608–617.

Tomura, M., Yoshida, N., Tanaka, J., Karasawa, S., Miwa, Y., Miyawaki, A., and Kanagawa, O. (2008). Monitoring cellular movement in vivo with photoconvertible fluorescence protein "Kaede" transgenic mice. Proc. Natl. Acad. Sci. USA *105*, 10871–10876.

Tränkner, D., Hahne, N., Sugino, K., Hoon, M.A., and Zuker, C. (2014). Population of sensory neurons essential for asthmatic hyperreactivity of inflamed airways. Proc. Natl. Acad. Sci. USA *111*, 11515–11520.

Trier, A.M., Mack, M.R., and Kim, B.S. (2019). The Neuroimmune Axis in Skin Sensation, Inflammation, and Immunity. J. Immunol. *202*, 2829–2835.

Tussiwand, R., Everts, B., Grajales-Reyes, G.E., Kretzer, N.M., Iwata, A., Bagaitkar, J., Wu, X., Wong, R., Anderson, D.A., Murphy, T.L., et al. (2015). Klf4 expression in conventional dendritic cells is required for T helper 2 cell responses. Immunity *42*, 916–928.

Usoskin, D., Furlan, A., Islam, S., Abdo, H., Lönnerberg, P., Lou, D., Hjerling-Leffler, J., Haeggström, J., Kharchenko, O., Kharchenko, P.V., et al. (2015). Unbiased classification of sensory neuron types by large-scale single-cell RNA sequencing. Nat. Neurosci. *18*, 145–153.

Van Dyken, S.J., and Locksley, R.M. (2018). Chitins and chitinase activity in airway diseases. J. Allergy Clin. Immunol. *142*, 364–369.

Veiga-Fernandes, H., and Mucida, D. (2016). Neuro-Immune Interactions at Barrier Surfaces. Cell *165*, 801–811.

Xu, J., Zanvit, P., Hu, L., Tseng, P.Y., Liu, N., Wang, F., Liu, O., Zhang, D., Jin, W., Guo, N., et al. (2020). The Cytokine TGF-beta Induces Interleukin-31 Expression from Dermal Dendritic Cells to Activate Sensory Neurons and Stimulate Wound Itching. Immunity *53*, 371–383.

Yosipovitch, G., Stander, S., Kerby, M.B., Larrick, J.W., Perlman, A.J., Schnipper, E.F., Zhang, X., Tang, J.Y., Luger, T., and Steinhoff, M. (2018). Serlopitant for the treatment of chronic pruritus: Results of a randomized, multicenter, placebo-controlled phase 2 clinical trial. J. Am. Acad. Dermatol. *78*, 882–891.

Zylka, M.J., Rice, F.L., and Anderson, D.J. (2005). Topographically distinct epidermal nociceptive circuits revealed by axonal tracers targeted to Mrgprd. Neuron *45*, 17–25.

STAR★METHODS

KEY RESOURCES TABLE

REAGENT or RESOURCE	SOURCE	IDENTIFIER
Antibodies		
Anti-mouse CD103, Clone:M290	BD Biosciences	Cat#: 740355; RRID: AB_2740087
Anti-mouse CD117(c-kit), Clone: 2B8	BioLegend	Cat#: 105839; RRID: AB_2629798
Anti-mouse CD117(c-kit), Clone: 2B8	BioLegend	Cat#: 105813; RRID: AB_313222
Anti-mouse CD117(c-kit), Clone: 2B8	BioLegend	Cat#: 105815; RRID: AB_493473
Anti-mouse CD11b, Clone: M1/70	BD Biosciences	Cat#: 553312; RRID: AB_398535
Anti-mouse/human CD11b, Clone: M1/70	BioLegend	Cat#: 101208; RRID: AB_312791
Anti-mouse CD11b, Clone: M1/70	BioLegend	Cat#: 101251; RRID: AB_2562904
Anti-mouse CD11b, Clone: M1/70	BioLegend	Cat#: 101217; RRID: AB_389305
Anti-mouse CD11b, Clone: M1/70	eBioscience	Cat#: 25-0112-82; RRID: AB_469588
Anti-mouse CD11c, Clone: HL3	BD Biosciences	Cat#: 562782; RRID: AB_2737789
Anti-mouse CD11c, Clone: HL3	BD Biosciences	Cat#: 553801; RRID: AB_395060
Anti-mouse CD11c, Clone: N418	BioLegend	Cat#: 117334; RRID: AB_2562415
Anti-mouse CD11c, Clone: N418	BioLegend	Cat#: 117353; RRID: AB_2686978
Anti-mouse CD273 (PDL2), Clone: TY25	BioLegend	Cat#: 107210; RRID: AB_2566345
Anti-mouse CD3, Clone: 17A2	BioLegend	Cat#: 100204; RRID: AB_312661
Anti-mouse CD3ε, Clone: 145-2C11	BioLegend	Cat#: 100351; RRID: AB_2565842
Anti-mouse CD301b (MGL2), Clone: URA-1	BioLegend	Cat#: 146808; RRID: AB_2563390
Anti-mouse CD4, Clone: GK1.5	BioLegend	Cat#: 100437; RRID: AB_10900241
Anti-mouse CD4, Clone: GK1.5	BioLegend	Cat#: 100451; RRID: AB_2564591
Anti-mouse CD4, Clone: RM4-5	BioLegend	Cat#: 100516; RRID: AB_312719
Anti-mouse CD4, Clone: GK1.5	BioLegend	Cat#: 100408; RRID: AB_312693
Anti-mouse/human CD44, Clone: IM7	BioLegend	Cat#: 103025; RRID: AB_493712
Anti-mouse CD45, Clone: 30-F11	BioLegend	Cat#: 103124; RRID: AB_493533
Anti-mouse CD45, Clone: 30-F11	BioLegend	Cat#: 103151; RRID: AB_2565884
Anti-mouse CD45.1, Clone: A20	BioLegend	Cat#: 110708; RRID: AB_313497
Anti-mouse CD45.2, Clone: 104	BioLegend	Cat#: 109818; RRID: AB_492870
Anti-mouse CD69, Clone: H1.2F3	BioLegend	Cat#: 104543; RRID: AB_2629640
Anti-mouse CD8α, Clone: 53-6.7	BioLegend	Cat#: 100722; RRID: AB_312761
Anti-mouse CD86, Clone: PO3	BioLegend	Cat#: 105106; RRID: AB_313159
Anti-mouse FcεRIα, Clone: MAR-1	BioLegend	Cat#: 134327; RRID: AB_2721324
Anti-mouse IL-4, Clone: 11B11	BD Biosciences	Cat#: 557728; RRID: AB_396836
Anti-mouse/human IL-5, Clone: TRFK5	BioLegend	Cat#: 504303; RRID: AB_315327
Anti-mouse IL-13, Clone: eBio13a	Invitrogen	Cat#: 25-7133-82; RRID: AB_2573530
Anti-mouse IFN-γ, Clone: XMG1.2	BioLegend	Cat#: 505810; RRID: AB_315404
Anti-mouse I-A[b], Clone: AF6-120.1	BD Biosciences	Cat#: 553552; RRID: AB_394919
Anti-mouse I-A/I-E (MHC II), Clone: M5/114.15.2	BioLegend	Cat#:107631; RRID: AB_10900075
Anti-mouse I-A/I-E (MHC II), Clone: M5/114.15.2	BioLegend	Cat#: 107635; RRID: AB_2561397
Anti-mouse I-A/I-E (MHC II), Clone: M5/114.15.2	BioLegend	Cat#:107626; RRID: AB_2191071
Anti-mouse Ly6G/Ly6C (Gr-1), Clone: RB6-8C5	BioLegend	Cat#: 108412; RRID: AB_313377
Anti-mouse Siglec-F, Clone: E50-2440	BD Biosciences	Cat#: 552126; RRID: AB_394341
Biotinylated anti-Tuj1	BD Biosciences	Cat#: BAM1195; RRID: AB_356859
Fixable Viability Dye eFluor 780	Invitrogen	Cat #: 65-0865-14
TruStain fcX anti-mouse CD16/32, Clone: 93	BioLegend	Cat #: 101320; RRID: AB_1574975

(*Continued on next page*)

Continued

REAGENT or RESOURCE	SOURCE	IDENTIFIER
Critical Commercial Assays		
Substance P ELISA Kit	Cayman Chemical Company	Cat #: 583751
CGRP (rat) EIA Kit	Cayman Chemical Company	Cat #: 589001
BD Cytofix/Cytoperm	BD Biosciences	Cat#: 554714; RRID: AB_2869008
RNeasy Plus Micro Kit (50)	QIAGEN	Cat #: 74034
RNeasy Plus Mini Kit (50)	QIAGEN	Cat #: 74134
Experimental Models: Organisms and Strains		
Mouse: C57BL/6	Charles River Laboratory	Strain No.: 027; RRID:IMSR_CRL:027
Mouse: C57BL/6	The Jackson Laboratory	Strain No.: 000664; RRID:IMSR_JAX:000664
Mouse: B6(FVB)-Mgl2$^{tm1.1(HBEGF/EGFP)Aiwsk}$/J (*Cd301b*^{DTR})	The Jackson Laboratory	Strain No.: 023822; RRID:IMSR_JAX:023822
Mouse: Kaede^{+}	Tomura et al., 2008	N/A
Mouse: NCI Br-Ly5.1/Cr	Charles River Laboratory	Strain No.: 564; RRID:IMSR_CRL:564
Mouse: *Mrgpra1*$^{-/-}$	Meixiong et al., 2019b	N/A
Mouse: *Nav1.8*^{cre}	Abrahamsen et al., 2008	N/A
Mouse: *Trpv1*^{DTR}	Pogorzala et al., 2013	N/A
Mouse: *tdTomato*^{loxSTOPlox} [Ai14]	The Jackson Laboratory	Strain No.: 007908; RRID:IMSR_JAX:007908
Mouse: B6.Cg-*Kit*$^{W-sh}$/HNihrJaeBsmJ (*Kit*$^{w-sh/w-sh}$)	The Jackson Laboratory	Strain No.: 030764; RRID:IMSR_JAX:030764
Mouse: B6.Cg-*Tac1*^{tm1Bbm}/J (*Tac1*$^{-/-}$)	The Jackson Laboratory	Strain No.:004103; RRID:IMSR_JAX:004103
Mouse: 4get	Mohrs et al., 2001.	N/A
Oligionucleotides for qPCR		
mMrgpra1 FWD (5′-GCAAGAGGAATGGGGGAAAGC −3′)	This manuscript	N/A
mMrgpra1 REV (5′-CCCGACCAGTCCGAAGATGAT −3′)	This manuscript	N/A
mMrgprb2 FWD (5′-ATCAAGAATCTAAGCACCTCAGC −3′)	This manuscript	N/A
mMrgpgrb2 REV (5′-GAAAGCAAAATCATGGCTTGGT −3′)	This manuscript	N/A
mTacr1 FWD (5′-CTTCACCTACGCAGTCCACAA,- 3′)	This manuscript	N/A
mTacr1 REV (5′-GGCTGAAGAGGGTGGATGATG −3′)	This manuscript	N/A
mTacr2 FWD (5′-GCTGACAGGTACATGGCCATTG −3′)	This manuscript	N/A
mTacr2 REV (5′ TGGAGTAGAAACATTGTGGGGAGG −3′)	This manuscript	N/A
mTrpv1 FWD (5′-CCACTGGTGTTGAGACGCC −3′)	This manuscript	N/A
mTrpv1 REV (5′TCTGGGTCTTTGAACTCGCTG-3′)	This manuscript	N/A
Chemicals, Peptides, & Recombinant Proteins		
TRIzol Reagent	Invitrogen	Ref #: 15596018
Triton X-100	Sigma-Aldrich	Cat#: T9284
Collagenase A	Sigma Aldrich	Cat#: 10103578001
Collagenase P	Sigma-Aldrich	Cat #: 11213857001
Dispase II	Sigma-Aldrich	Cat #: D4693-1G

(*Continued on next page*)

Continued

REAGENT or RESOURCE	SOURCE	IDENTIFIER
DNase I, grade II	Sigma-Aldrich	Cat #: 10104159001
Dnase I Type IV	Sigma-Aldrich	Cat#: D5025
Liberase	Sigma-Aldrich	Cat #: 05401119001
Cytosine beta-D-arabinofuranoside	Sigma-Aldrich	Cat#: C6645
B-27 Supplement (50X)	Thermo Fisher Scientific	Cat#: 10889038
GlutaMAX	GIBCO	Cat#: 35050061
Laminin	Sigma-Aldrich	Cat#: L2020
GDNF	Sigma-Aldrich	Cat#: G1401
Nerve Growth Factor 2.5S	Invitrogen	Cat#: 13257019
Papain	Sigma-Aldrich	Cat: 5125
Ovalbumin	Sigma-Aldrich	Cat: A5503
LPS	Invivogen	Cat: tlrl-eklps
Capsaicin	Sigma-Aldrich	Cat#: M2028
Histamine	Sigma-Aldrich	Cat#: H7125
Phospholipase A_2	Sigma-Aldrich	Cat #: P9279
Alternaria alternata	Greer Laboratories Inc	Cat#: NC1620293
Mite, House dust	Greer Laboratories Inc	Cat#: NC9756554
Calcitonin Gene Related Peptide (CGRP) powder	Sigma-Aldrich	Cat#:C0292-1MG
Substance P	Tocris	Cat#: 1156
QX314 chloride	Tocris	Cat#: 2313
QWF	Tocris	Cat#: 6642
L733,060 hydrochloride	Tocris	Cat#: 1145
Chloroquine diphosphate	Sigma-Aldrich	Cat#: C6628
Potassium chloride solution, 3M	Sigma-Aldrich	Cat#: 60137
Nle-Arg-Phe amide (FMRF)	Sigma Aldrich	Cat#: N3637
Normal Goat serum (NGS)	Jackson Immunoresearch	Cat#: 005-000-121
DMEM	N/A	N/A
Krebs-Ringer Bicarbonate Buffer	Boston Bioproducts	Cat#: BSS-250
PBS	Corning	Ref #: 21-031-CV
Fura-2, AM	Thermo Fisher Scientific	Cat #: F1201
Red blood cell lysis buffer	Sigma-Aldrich	Cat #: R7757
0.5 M EDTA, pH 8.0	GIBCO	Cat #: 15575-038
OCT Compound	Tissue-Tek	Cat #: 4583
DMEM	Corning	10-014-CV
RPMI 1640, 1X	Corning	Ref #: 15-040-CV
Neurobasal-A Medium	Thermo Fisher Scientific	Cat #: 10888
Fetal Calf Serum (FCS)	Atlanta Biologicals	Cat #: S11550
MultiScribe Reverse Transcriptase	Thermo Fisher Scientific	Ref #: 4311235
GeneAMP dNTP mix with dTTP	Thermo Fisher Scientific	Ref #: N8080260
$MgCl_2$ Solution 25 mM	Thermo Fisher Scientific	Ref #: 4486224
10x PCR Buffer II	Thermo Fisher Scientific	Ref #: 4486220
Oligio d(T)16	Thermo Fisher Scientific	Ref #: 100023441
Random Hexamers 50 μM	Thermo Fisher Scientific	Ref #: 100026484
RNase Inhibitor	Thermo Fisher Scientific	Ref #: 100021540
FastStart Essential DNA Green Master	Roche	Cat #: 25595200
Software		
Prism v 7.0c	GraphPad	https://www.graphpad.com/demos

(*Continued on next page*)

Continued

REAGENT or RESOURCE	SOURCE	IDENTIFIER
Zen Blue	Zeiss	https://www.zeiss.com/microscopy/us/products/microscope-software/zen.html
Imaris	Bitplane	http://www.bitplane.com/download
Softmax Pro	Molecular Devices	https://www.moleculardevices.com/systems/microplate-readers/softmax-pro-7-software
BD FACS Diva 8	BD Biosciences	http://www.bdbiosciences.com/us/instruments/clinical/software/flow-cytometry-acquisition/bd-facsdiva-software/m/333333/overview
FlowJo (version 10)	Tree Star	https://www.flowjo.com/solutions/flowjo/downloads

RESOURCE AVAILABILITY

Lead Contact

Further information and requests for resources and reagents should be directed to and will be fulfilled by the Lead Contact, Caroline L. Sokol (CLSOKOL@mgh.harvard.edu).

Materials Availability

This study did not generate new unique reagents or animal strains.

Data and Code Availability

This study did not generate any unique datasets or code.

EXPERIMENTAL MODEL AND SUBJECT DETAILS

Mice

All animal experiments were approved by the Massachusetts General Hospital or Harvard Medical School Institutional Animal Care and Use Committee (IACUC). Mice were bred and maintained in a specific-pathogen-free (SPF) animal facility at Massachusetts General Hospital. C57BL/6, *Kit*$^{W\text{-}sh/W\text{-}sh}$, Ly5.1, and *Tac1*$^{-/-}$ mice were purchased from Charles River Laboratories (Wilmington, MA) or Jackson Laboratories (Bar Harbor, ME). *Nav1.8*^{cre} mice were originally from Dr. John Wood (University College London), and *Trpv1*^{DTR} from Dr. Mark Hoon (NIH). Kaede mice were originally from Osami Kanagawa and were crossed with *Trpv1*^{DTR} mice to generate Kaede *x Trpv1*^{DTR} mice. *Nav1.8*^{cre} mice were crossed with *tdTomato*^{loxSTOPlox} to generate *Nav1.8*^{tdTomato} mice. 4get (IL-4-eGFP) mice on a C57BL/6 background were provided by Markus Mohrs. Bone marrow from *Mrgpra1*$^{-/-}$mice on a C57BL/6 background was kindly provided by Dr. Xinzhong Dong (Johns Hopkins, MD). Mice were used in experiments at 5-14 weeks of age. Sex and age-matched littermates or purchased C57BL/6 mice were used as wild-type controls. Both female and male mice were used for all experiments and numbers were matched among the experimental conditions.

Experimental Mouse Models

Diphtheria Toxin Depletion

C57BL/6, *Trpv1*^{DTR}, Kaede, or Kaede x *Trpv1*^{DTR} mice were injected intraperitoneally (i.p) with 0.2 μg of DT (Sigma-Aldrich) daily for 5 days then rested for 2 days repeated over a 21 day period. Mice rested for seven days after the final DT injection. Effective depletion was confirmed through tail flick assay and qPCR of DRGs. For the tail flick assay, the tail of each mouse was placed into 52°C water for a maximum of ten seconds, or less if mouse removed the tail from water. For CD301b+ DC depletion in epicutanous immunization experiments, following depilation of fur on the tail flank skin of wild-type and *Cd301b*^{DTR} mice, 0.5 μg of DT in 100 μL PBS was injected intraperitoneally for three consecutive days. The epicutaneous patch was applied on the third day of DT injections. For BM chimera experiments, mice were injected with 0.5 μg of DT in 100 μL PBS on two consecutive days. On the second day of DT injection, mice were also immunized with OVA or OVA & papain, then euthanized 24 h later for analysis of DC migration.

Kaede Photoconversion

A 2 × 2 cm patch of skin above the base of tail was shaved followed by application of a chemical depilatory agent (Veet) for 1 min, then removed by multiple washings with PBS. The exposed skin was subjected to violet light (420 nm) using a Bluewave LED visible light curing unit (Dymax) with a 420 nm bandpass filter (Andover Corp). Skin was exposed to this wavelength with the light source at a maximum power, approximately 7.5 cm away from the skin for 5 min. Following photoconversion, mice were immunized

intradermally or epicutaneously in the shaved region as described above. 24 h following immunization, dLNs were isolated and analyzed for skin DC migration using flow cytometry.

Bone Marrow Chimera Generation

Donor bone marrow (BM) was extracted from femurs and tibias of mice using a mortar and pestle. BM cells were incubated in red blood cell lysis buffer (Sigma-Aldrich), then the purified BM cells were resuspended in 1x PBS. $10x10^6$ BM cells in 100 μL of PBS were intravenously injected into lethally irradiated (1000 rads) C57BL/6 recipients within 3 h of irradiation. For comparative migration experiments, recipient WT mice received a 1:1 mix of WT/*Cd301b*^{DTR} BM (CD301b^{WT} mice) or *Mrgpra1*$^{-/-}$/*Cd301b*^{DTR} BM (CD301b$^{Mrgpra1-/-}$ mice). Recipient mice were rested for 6-8 weeks, then injected intraperitoneally with 0.5 μg diphtheria toxin (DT). 24 h later, mice were again injected intraperitoneally with 0.5 μg DT followed by intradermal footpad injections with 50 μg OVA in the right footpad and 50 μg OVA + 50 μg papain in the left footpad. 24 h later, the dLN was harvested for assessment of CD301b$^+$ DCs by flow cytometry. For competitive migration experiments, recipient WT mice received a 1:1 mix of CD45.1 WT/CD45.2 *Mrgpra1*$^{-/-}$ BM. Recipient mice were rested for 6-8 weeks, then intradermally injected with 50 μg OVA + 50 μg papain or 50 μg OVA + 10 μg LPS in bilateral footpads. 24 h later, the dLN and ear skin was harvested for chimeric assessment of CD11c$^+$CD301b$^+$ DCs (OVA & papain) or CD11c$^+$CD103$^+$ DCs (OVA & LPS) by flow cytometry.

Cell or Tissue Isolation and Culture

Both female and male mice were used for all cell and tissue culture experiments and numbers were matched among the experimental conditions.

Dorsal Root Ganglia Cultures and Stimulation

Dorsal root ganglia (DRGs) were harvested from mice (7-14 weeks old) and dissected into DMEM supplemented with 0.1% glucose, 0.1% L-glutamine, 0.1% sodium pyruvate (Corning) with added 10% heat inactivated FBS (Sigma-Aldrich) and 1% Pen/Strep (Lonza). DRGs were then dissociated in 1.25 mg/mL Collagenase A (Roche) + 2.5 mg/ml Dispase II (Sigma-Aldrich) in 1x PBS (Corning). Dissociated DRGs were washed in supplemented DMEM and were triturated using needles of different sizes (18G, 21G, 26G, six times each) in Neurobasal-A medium (Invitrogen) supplemented with B27 (Invitrogen), 1% GlutaMAX, and 1% Pen/Strep, with added growth factors 0.01 mM arabinocytidine (Ara-C), 0.002 ng/μL glial derived neurotrophic factor (GDNF) (Sigma-Aldrich) and nerve growth factor 2.5S (NGF 2.5S) (Invitrogen). For culture in a 96-well sterile tissue-culture (TC) treated plate (Corning), around 12,000 DRG neurons/well were plated at a standard 30 μL/well into 10 μg/ml laminin (Sigma-Aldrich) pre-coated plates and incubated for 1 h at 37°C in a CO_2 tissue incubator (Thermo Scientific). After the one-hour incubation, 100 μL of supplemented Neurobasal-A medium with added growth factors was added to each well. The DRGs incubated for 24 h. For stimulations, media was replaced with 200 μL/well of supplemented Neurobasal-A medium without the addition of growth factors and DRG neuron cultures were either left unstimulated with vehicle control (PBS) or stimulated with papain, heat-inactivated papain, increasing concentrations (100 μg/mL, 150 μg/mL, or 200 μg/mL) of Alternaria extract or HDM extract for 1 h. Supernatant was used for further analysis.

Flank Explant Assay

Wild-type mice were shaved at the flanks and injected as described. Mice were immediately sacrificed and punch biopsies of the shaved flanks were collected and rapidly transferred into a 24-well plate containing 1 mL of serum free DMEM. Explants were incubated for 30 min at 32°C with gentle rotation (150 rpm) before supernatants were collected for analysis.

Generation of Bone Marrow-derived Dendritic Cells (BMDCs)

BM was harvested from 5- to 8-week-old mice by mechanical disruption using a mortar and pestle, followed by incubation with red blood cell lysis buffer (Sigma-Aldrich). BM cells were cultured in growth media supplemented with 10% HI FBS (Sigma-Aldrich), 1% Pen/Strep (Lonza), 1% GlutaMAX(GIBCO), 1% HEPES buffer (Corning), 1% Non-Essential Amino Acid Solution (Lonza), 1% Sodium Pyruvate (GIBCO), 0.1% 2-mercaptoethanol (GIBCO), with 20 ng/mL of granulocyte-macrophage colony-stimulating factor (GM-CSF) (Peprotech) at a density of 0.7×10^6 cells/mL, fed on days 2 and 4 and stimulated on day 5 of culture.

Stimulation of Primary Dendritic Cells

Skin draining lymph nodes from naive C57BL/6 mice were harvested and digested as described in *Flow cytometry and Cell sorting*. Cell suspensions underwent MACS-mediated CD11c positive selections (Miltenyi) followed by overnight stimulation with heat inactivated papain (100 μg/ml), papain (100 μg/ml), or LPS (100 ng/ml) at $1x10^6$ cells per ml in fully supplemented RPMI with 10% heat inactivated fetal bovine serum. Cells were harvested and processed for flow cytometric analysis.

METHOD DETAILS

Intradermal Immunizations

Mice were immunized intradermally (i.d) in the right side of the cheek (behavioral experiments), base of tail (Kaede experiments), or in footpads. As indicated, mice were immunized with 50 μg of papain, heat-inactivated papain, ovalbumin, histamine, or 40 μg of Capsaicin (all from Sigma-Aldrich); or 100 μg of Alternaria alternata (Greer). Where indicated, mice were injected with 10 μg LPS

(InvivoGen), 5 μg CGRP (Sigma-Aldrich), 100 nmoles Substance P (Tocris) or 1% QX314 (Tocris). All dilutions were diluted in sterile 1x phosphate buffered saline, or PBS (Corning), except for capsaicin which was diluted in PBS and 6.4% DMSO. Where indicated, immunizations were performed with either 500 μmol of QWF or L733060 (both from Tocris) diluted in a 5% DMSO PBS solution.

Epicutaneous Sensitization

Mice were shaved and depilated (Veet) on their back two days before a 1cm x 1cm gauze soaked in 100 μl of 2 mg/ml OVA in PBS, Papain in PBS, or PBS alone was placed on the back skin near the base of the tail and covered with a waterproof transparent adhesive film (Flexigrid, Smith and Nephew Opsite) for 24 h.

Behavioral Analysis

For pain and itch assays, mice were allowed to acclimate to cage apparatus for 2 h prior to filming, with food and water provided. A white noise machine (Marpac) was used to reduce distractions from behavioral response. After habituation, mice were immunized i.d. in the right cheek with substances administered in a 25 μL vehicle under brief isoflurane anesthesia. Mice were videotaped in isolation for 20 min. Videos were then examined for quantification of wiping (single ipsilateral paw to injected cheek) and scratching (ipsilateral hind paw to injected cheek). Data were quantified in five-minute intervals.

Calcium Imaging of DRG Neuronal Cultures

DRGs were harvested and digested in a mix of Collagenase A (2.5 mg/ml) and Dispase II (1 mg/mL) for 80 min while shaking at 37°C, DRGs were then resuspended in DMEM/F12 (Thermo Fisher) and mechanically triturated using needles of different sizes (18G, 21G, 26G, six times each). The cell suspension was carefully plated on laminin precoated 35 mm plates in DMEM/F12 supplemented with NGF 25 ng/mL and GDNF 2 ng/mL and cultured overnight.

For calcium imaging, cells were loaded with 5 μM Fura-2-AM / DMEM/F12 (Thermo Fisher) at 37°C for 30 min, washed 3x, and imaged in 2 mL Krebs-Ringer solution (Boston Bioproducts) (KR: 120 mM NaCl, 5 mM KCl, 2 mM $CaCl_2$, 1 mM $MgCl_2$, 25 mM sodium bicarbonate, 5.5 mM HEPES, 1 mM D-glucose, pH 7.2 ± 0.15). 100 μg papain or vehicle (PBS) stimulation was followed by 100 μM histamine, 1 mM chloroquine, 1 μM capsaicin and 80 mM KCl sequentially applied to identify shared neuronal responses of itch sensitizing stimulants. Images were acquired with alternating 340/380 nm excitation wavelengths, and fluorescence emission was captured using a Nikon Eclipse Ti inverted microscope and Zyla sCMOS camera (Andor). Ratiometric analysis of 340/380 signal intensities were processed, background corrected, and analyzed with NIS-elements software (Nikon) by drawing regions of interest (ROI) around individual cells as also previously described (Lai et al., 2020).

Each neuron was analyzed for excitability with an increase from baseline greater than 15% considered to be a positive response. All neurons responding to KCl are considered viable and potentially excitable. With that as a baseline, the subsequent percentages of papain, histamine, chloroquine, capsaicin, and vehicle responsive cells were quantified and plotted as proportion of KCl responsive cells. Response traces of single DRG neurons were generated using Microsoft Excel. Venn Diagram showing the numbers of individual neurons responding one or more stimulants was created using R studio 3.6.2. Violin plots were created using GraphPad PRISM software 8.4.

Microscopy and Image Quantification

Ears were harvested, split into dorsal and ventral halves, removed of hair (Veet) and placed on Flexigrid transparent adhesive film (Smith and Nephew Opsite) dermal side up. Fat was gently removed and each tissue sample was floated on 3 mL of DMEM (Corning) supplemented with 3 mg/mL Dispase II (Sigma-Aldrich) per well of a 6-well plate, dermal side down, for 90 min at 37°C in 5% CO_2. Afterward, the samples were dried and the dermal tissue was gently peeled away from the epidermal tissue. Dermal slices were then isolated, rinsed in PBS, and fixed in a 4% paraformaldehyde (Electron Microscopy Sciences) PBS solution for 1 hour at 4 °C. After washing in PBS, samples were incubated overnight with a primary antibody solution of biotinylated anti-Tuj1 (BD Biosciences) diluted in PBS with 0.2% Triton X-100 (Sigma-Aldrich) and 10% heat inactivated goat serum (Jackson ImmunoResearch). Samples were washed 3 times for 10 min in PBS with 0.2% Triton X-100 and 2% heat inactivated goat serum and then stained with Streptavidin-AF488, CD301b-AF647, and MHCII-BV421 (all from BioLegend) diluted in PBS with 0.2% Triton X-100 and 10% heat inactivated goat serum for 1 h at room temperature with shaking. Washed ears were mounted using Prolong Diamond Antifade Mountant (Thermo Fisher Scientific) prior to imaging on a Zeiss LSM confocal microscope. Images were analyzed using Zen Blue to quantify the distance of $MHCII^+CD301b^+$ cells and $MHCII^+CD301b^-$ cells from their nearest $Nav1.8^+$ neuron as measured in 3D Ortho.

Enzyme-Linked Immunosorbent Assay (ELISA)

Mouse Substance P and CGRP were detected using competitive mouse Substance P and CGRP ELISA kits (both from Cayman Chemical). All procedures were carried out according to the manufacturer's protocols. Samples were assayed on Softmax Pro Software in duplicates and concentrations were determined from a standard curve.

Flow Cytometry and Cell Sorting

Harvested lymph nodes were subjected to digestion at 37°C in DNase I (100 μg/mL, Roche), Collagenase P (200 μg/mL, Sigma-Aldrich), Dispase II (800 μg/mL, Sigma-Aldrich), and 1% fetal calf serum (FCS) in RPMI. At 7 min intervals, supernatant was removed and replaced with fresh enzyme media until no tissue fragments remained. Supernatant was added to added to stop buffer

(RPMI/2mM EDTA (GIBCO)/1% FBS) and filtered prior to antibody staining. To analyze the cells of skin, ears were harvested and forceps were used to separate the dorsal and ventral halves. The epidermis was attached to Flexigrid transparent adhesive film (Smith and Nephew Opsite), then ear halves were floated dermis side down in Dispase II (3 mg/mL, Sigma-Aldrich) in DMEM for 90 min at 37°C in 5% CO_2. The dermis was then removed from the epidermis, which remained on the Flexigrid tape. The epidermis was digested in Collagenase IV (2 mg/mL, Sigma-Aldrich) in DMEM, while the dermis was digested in Liberase TM (25 μg/mL, Sigma-Aldrich), DNase I (75 μg/mL, Sigma-Aldrich), and 10 μM HEPES (Corning) in DMEM. The dermis and epidermis were digested for 45 min at 37°C in 5% CO_2; tubes containing the dermal and epidermal samples were vigorously shaken every 9 min. Following digestion, 500 μL of 15 μM EDTA (GIBCO) in heat inactivated FBS (Sigma-Aldrich) was added to each sample. The dermis was subjected to gentleMACS dissociation, then dermal and epidermal cell suspensions were combined and filtered before antibody staining. Enzymatically digested cell suspensions were incubated for 15 min at 4°C in PBS with 0.5% FCS with the fluorophore-conjugated antibodies.Intracellular cytokine staining was performed after PMA/Ionomycin (Sigma) stimulation of single cell suspensions in the presence of GolgiPlug for 4 h prior to intracellular staining using BD Cytofix/Cytoperm kit (BD Biosciences). Viability was determined using Fixable Viability Dye eFluor 780 (Invitrogen). Samples were processed on a Beckman Coulter CytoFLEX S, BD Fortessa X20, or BD FACSAria Fusion and analyzed using FlowJo (Version 10) (TreeStar).

Quantitative PCR (qPCR)

Total RNA from sorted cells, DRGs, or BMDCs was isolated using the QIAGEN RNeasy Micro Kit in accordance with the manufacturer's protocol. 50 μL of cDNA per reaction was generated using random hexamers, Oligo (dT), magnesium chloride, dNTPs (10 mM), Reverse Transcriptase, and RNase inhibitor (all from Thermo Fisher Scientific). A Roche LightCycler 96 Real-Time PCR System was utilized to quantify gene expression, with SYBR Green Master Mix (Roche). The reaction cycles were: 95°C for 600 s, then 95°C, 60°C, and 72°C for 10 s each for 45 total cycles, followed by 95°C for 10 s, 65°C for 60 s, and finally 97°C for 1 s. Fluorescence was quantified during each amplification. Quantification cycle (Cq) values for each sample were determined using Roche LightCycler 96 Software 1.1. Microsoft Excel was used to determine copy values for Cq in order to divide by *Gapdh* copy values for ratio analysis.

Chemotaxis Assays

On day 5 of culture, BMDCs were stimulated with: LPS (100 ng/mL, InvivoGen), papain (100 μg/mL, Sigma-Aldrich), Substance P (0.5 μM, Sigma-Aldrich), Nle-Arg-Phe amide, or FMRF (30 μM, Sigma-Aldrich). Cells were then harvested. Chemotaxis was performed on these harvested cells using 5 μm pore size Transwell membranes (NeuroProbe). 32 μL of CCL21 (100 ng/mL) or media alone with 0.5% BSA in RPMI, were added to the wells of the lower chamber. The Transwell membrane was then outfitted to the microplate, after which 100,000 cells in 50 μL of chemotaxis media were added in triplicate. Plates were incubated for 2 hr at 37°C in 5% CO_2. Afterward, the membrane was quickly rinsed with sterile PBS and spun down for 1 min at 1500 rpm to collect any migrated adherent cells. The membrane was then removed, and migrated cells were counted.

QUANTIFICATION AND STATISTICAL ANALYSIS

Statistical analysis of results was performed using GraphPad Prism 7-8 (GraphPad Software). Unpaired t test, ordinary one-way ANOVA, or two-way ANOVA were applied as indicated in figure legends. Statistical significance was considered for p-values < 0.05. Details are listed in the respective figure legends.